Energy, Mines and Resources Canada | Énergie, Mines et Ressources Canada

CANMET

Canada Centre for Mineral and Energy Technology | Centre canadien de la technologie des minéraux et de l'énergie

POST-FAILURE MULTI-STAGE TRIAXIAL STRENGTH DETERMINATIONS USING A COMPUTER CONTROLLED SERVO-HYDRAULIC TEST SYSTEM

B. Gorski

CANADIAN MINE TECHNOLOGY LABORATORY

APRIL 1987

MINING RESEARCH LABORATORIES

DIVISIONAL REPORT MRL 87-4 (TR)

MRL 87-4(TR)c.2

POST-FAILURE MULTI-STAGE TRIAXIAL STRENGTH DETERMINATIONS USING A COMPUTER CONTROLLED SERVO-HYDRAULIC TEST SYSTEM

B. Gorski*

Abstract

Post-failure, multi-stage triaxial compressive strength tests were conducted on granite and diabase specimens. The test program was undertaken to determine if the newly acquired computer controlled servo-hydraulic test system has the capability to control rock specimen failure into the post-peak strength region. Rock specimens known to exhibit Class II failure characteristics in the post-failure region were selected for this test program. The results of the test are presented in this report.

*Rock Mechanics and Development Technologist, Canadian Mine Technology Laboratory (CMTL), Mining Research Laboratories, CANMET, Energy, Mines and Resources Canada, Ottawa.

MESURE DE LA RÉSISTANCE À LA COMPRESSION TRIAXIALE À PLUSIEURS ÉTAGES, DES ÉCHANTILLONS DE ROCHE, SUITE À LA RUPTURE, AU MOYEN D'UN SYSTÈME DE CONTRÔLE AUTOMATISÉ À SERVOCOMMANDE HYDRAULIQUE

B. Gorski*

Résumé

Des essais de résistance à la compression triaxiale à plusieurs étages ont été menés sur des échantillons de granite et de diabase, suite à la rupture. Le programme d'essais visait à déterminer si le système automatisé à servocommande hydraulique utilisé pour les essais est capable de contrôler la résistance résiduelle des échantillons de roche dans la zone de résistance maximale. Des échantillons de roche dont les caractéristiques de rupture (classe II) étaient reconnues, ont été choisis pour le programme d'essais dont les résultats sont présentés dans le présent rapport.

*Technologue du développement de la mécanique des roches, Laboratoire canadien de technologie minière (LCTM), Laboratoires de recherche minière, CANMET, Énergie, Mines et Ressources Canada, Ottawa.

CONTENTS

TABLES

APPENDICES

1. INTRODUCTION

An increasing portion of Canadian underground mining in the future will take place under high ground stresses. For such conditions, the post-failure strength and deformational properties of the rock materials must be taken into consideration in design. The objective of the completed test program was to establish the capability of the newly acquired computer controlled servo-hydraulic test system to carry out rock specimen failure studies into the post-peak strength region.

Rock types have been divided into two classes depending on the basis of their stress-strain behaviour in the post-failure region under uniaxial loaded conditions (1). Class I behaviour is characterized by 'stable' fracture propagation, in the sense that work must be done on the sample to effect a further reduction in load-carrying ability. Hence rocks that exhibit Class I behaviour retain some strength, even after the compressive strength has been exceeded. Class II rock failure behaviour is self-sustaining, i.e., the elastic strain energy stored in the sample when the applied stress equals the compressive strength is sufficient to maintain fracture propagation until the specimen has lost virtually all strength. Fracture can be arrested only if strain energy is extracted from the test specimen during fracture propagation. It can be concluded, therefore, that Class II failure behaviour cannot be accommodated by simply stiffening a testing machine; fractures would propagate even if a machine's stiffness were infinite. However, Class II type rocks under triaxial loading conditions can exhibit a transition from brittle to ductile behaviour, and become fully ductile at some value of confining pressure. Rock types known to exhibit Class II failure characteristics in the post-failure region were selected for this test program.

The evaluation and proposed adaptation of equipment and development of testing procedures to meet analytic requirements concerning post-failure rock deformational proportions are described by Gyenge (2). The experimental techniques, testing procedures and special equipment used previously for determining the complete stress-strain behaviour of specimens of both hard and soft rock are described by Gorski (3,4).

CMTL recently acquired a MTS 815 Rock Mechanics Test System. The servo-hydraulic system was installed during December of 1986. Contractual on-site performance tests were completed during February of 1987. The MTS test system replaces the existing out-dated Tinius Olsen test system. The MTS test system increases both the type and the load range of rock mechanics tests which can be carried out by CMTL.

The MTS test system incorporates closed loop servohydraulics to control post-peak failure of Class II rock specimens. The required response time of the servo-controller system, used

for closed loop control, is dependent on the stiffness of the loading frame, and the rate of failure propagation within the rock specimen. The best test results are obtained with test systems possessing the faster control loops and stiffer frames.

The closed loop servohydraulic MTS test system is capable of monitoring changes in load, circumferential displacement, and axial displacement. Any one or a combination of these parameters may be measured with an appropiate transducer and used as the feedback signal in the control loop. The feedback signal becomes the independent variable for test control. The servo-controller compares the feedback signal with a program signal provided by a digital programmable function generator and provides an error signal proportional to the difference between them. The error signal is amplified to become the servovalve command signal. The load frame actuator is driven in the appropiate direction to reduce the error to zero.

Load is not a satisfactory feedback signal for post-failure testing of either Class I or Class II type rocks. Using load as a feedback parameter will not permit the control of a test beyond the maximum load carrying capability of the specimen. At that point, the programmed load will exceed the specimen strength and there will be a sudden complete failure as the loading actuator tries to maintain load.

Axial strain control is suitable for controlling post-failure tests of Class I rocks, when the axial strain following specimen failure increases monotonically. However, even for this purpose it is not the most sensitive feedback mode because axial strains are relatively small during the early stages of specimen crack formation. Loading a Class II specimen under axial strain control beyond peak strength will result in sudden failure, in a manner similar to the case when a load control test is used. In this case, loss of control results from a decrease in axial strain following peak strength; continued control requires a monotonically increasing axial strain.

The use of a circumferential transducer as the feedback signal for control provides the most sensitive means of detecting specimen failure. Formation of cracks at failure causes much more lateral strain than axial displacement. More importantly, for Class II failure behaviour, circumferential strain normally provides a reliable monotonically increasing relationship and analog signal for failure control. The specimen thus is controlled to dilate uniformly while load and axial strain can be monitored independently as failure progresses. The circumferential control mode was used successfully in a uniaxial post-failure test program completed in March of 1987 (5).

In this report, the experimental techniques and testing procedures used for determining

the complete stress-strain behaviour of BX size rock specimens are described. The testing procedure used is described by Kovari and Tisa (6). The multi-stage triaxial test program was completed in April of 1987 using the MTS test system.

2. TEST EQUIPMENT

The MTS test system comprises many hydraulic, mechanical and electronic components. The individual components are described in detail by Gorski (5). The components used for this test program will be described briefly as to their function.

MTS 315.03S Load Frame

The load frame is of fixed crosshead design and is rated at 4.5 MN for compressive load. The actuator is double-acting, servo-hydraulic and has a maximum stroke of 100 mm. The actuator is equipped with a Linear Variable Differential Transducer for stroke control and a Delta p Pressure Transducer for load control. Two 5 GPM servo-valves and a hydraulic service manifold control the actuator hydraulic fluid flow.

MTS 657 Triaxial Cell

The triaxial cell is rated up to 150 MPa and up to 200 ° C. The cell is equipped with a 2.22 MN rated load cell, 3 Linear Variable Differential Transducers (LVDT), endcaps, heat shroud, heater, permeability porting, thermocouples, circumferential extensometer and a hydraulic lift mechanism. Feedthroughs are provided for all electrical signals including two spare strain channels. The load cell may be used for load control and 3 LVDT units used for stroke control. The triaxial cell can accommodate rock specimens with dimensions up to 100 mm in diameter and 200 mm in length. Specimens are jacketed in teflon tubes.

MTS Confining Pressure Subsystem

Confining pressure is generated by using a 150 MPa rated intensifier with 1150 cm^3 high pressure displacement output. The intensifier is equipped with two 5 GPM servo-valves, hydraulic service manifold, pressure transducer for control and monitoring of confining pressure, DC displacement transducer and a reservoir for confining fluid.

MTS 448.85 Controller

The controller provides all the controls necessary for conducting manual and computer-controlled tests. Control may be selected with load, circumferential displacement or stroke as the independent variable. Adjustments to DC or AC conditioners may be made or

reconfigured. The DC error may be zeroed. Valve balance and dither may be adjusted. Control modes may be offset or interlocks enabled. Signals may be output to external devices. One of four different ranges may be selected for any one of the three control mode conditioners.

MTS 458.20 Micro-Console

Two micro-consoles are provided. One is for the confining pressure subsystem and the other is for the permeability pressure subsystem. The micro-consoles function basically the same as the MTS 448.85 controller. For either system, intensifier stroke or pressure may be selected as the control mode. The confining pressure micro-console houses the AC conditioners for the three axial linear variable differential transducers.

DEC Micro PDP 11/73 Computer

The computer comes equipped with a 512 kilobyte MOS memory, a RD51 10 mega - byte Winchester disk and a RX50 Dual 400 kilobyte floppy disk drive. Peripherals include two DEC VT240 graphics terminals, a DEC LA50 printer and a DEC LVP16 digital pen plotter.

MTS 468.20 Test Processor

The test processor contains devices used to provide computer controlled operation of the MTS servo-hydraulic test system. With built-in software the functions provided are: command signal generation; data acquisition and handling; monitoring and control of the operation of other system components; initiation of computer interrupt routines upon the detection of certain programmed events; and communication with the system controller and associated system control hardware.

3. TEST PROCEDURE

Specimen Selection

Multi-stage tests were conducted on 9 rock specimens: 4 granite specimens originated from Pinawa, Manitoba (7); 3 granite specimens originated from Atikokan, Ontario (7); and 2 diabase specimens from Lac Saint Jean, Quebec (8). Specimen selection data are listed in Table 1.

Specimen Preparation

Rock core specimens selected for triaxial tests were prepared with a length to diameter ratio of 2:1. All specimens were lapped to within the specified tolerances, oven-dried, weighed and dimensioned. The specimen preparation was performed according to the procedures used at MRL (3,9).

Multi-Stage Triaxial Test

Test specimens were loaded through failure using the MTS test system. All tests were performed in computer control. Initially the specimens were uniaxially loaded in load mode at a rate of 1 kN per second. When the load reached a value of 75% of the estimated failure load, 30% of the applied load was automatically removed. The test was then continued in circumferential extensometer control mode. The test specimens were circumferentially strained at a rate of 1 mm per 10 minutes to 3.8 mm maximum. Upon detecting the onset of failure in the uniaxial state, confinement pressure of the first stage was automatically applied to the specimen and the test was continued in the triaxial state. Each specimen was tested at 6.9 MPa, 13.8 MPa, 20.7 MPa, 27.6 MPa and 34.5 MPa confining pressures. Once residual strength was established at 34.5 MPa confining pressure, the test was switched from circumferential extensometer control mode to axial stroke control mode. The specimen was then displaced axially a further 0.5 mm in 60 seconds and the confinement pressure was reduced to zero at the same time and rate. The corresponding peak and residual strength values were obtained by the method established by Kovari and Tisa (6).

Data Acquisition/Reduction

Data was scanned and stored by the computer every 3 seconds. Signals from the load cell, circumferential extensometer, LVDT #1, confinement pressure and confinement intensifier ram stroke were scanned. Real time plotting of load versus axial displacement was obtained using a HP7046B X Y1 Y2 pen recorder wired to the MTS 448.85 controller.

The raw signals were reduced to engineering units and stored on a hard disk for later recall. Measurements from LVDT #1 were also corrected for end platen compression in the sensing gauge length. Reduced data was transferred to a VAX 750 computer for determination of specimen material constants. Mohr envelope plots were obtained using a laser printer.

Hard copy plots of test results for report purposes were obtained using the DEC LVP16 pen plotter. The DEC LA50 printer was used to provide hard copies of reduced data for analyses.

4. TEST RESULTS

Uniaxial Compressive Strength

The uniaxial compressive strength results, Q_u, are listed in Table 2. The specimen location, dimensions and density, of each tested specimen are listed in Table 1.

The stress-strain curve plots, of each test, are provided in Appendix B. Signals from LVDT #1 were used for strain measurement. Appendix C provides the stress-strain curve plots of each compressive test. Signals from a circumferential extensometer, located at mid-height of the specimen, were used for strain measurement. Appendix D provides the stress-confinement pressure plots.

The peak strain values, ϵ_{peak}, listed in Table 2, were determined from LVDT #1 readings.

Elastic Constants

The modulus of elasticity, E, was established in each uniaxial compressive test case. The obtained results are listed in Table 2. Young's modulus was determined using the tangent modulus at 50% of the compressive strength. Values of E were determined using signals from LVDT #1. The values used were from the load control mode part of the stress-strain curves.

Triaxial Compressive Strength

The triaxial compressive strengths of the specimens were determined at successive confining stages of: 6.9 MPa, 13.8 MPa, 20.7 MPa, 27.6 MPa and 34.5 MPa. The stress-strain plots of the multi-stage triaxial tests are provided in Appendices B and C. The results of the multi-stage tests are tabulated in Table 2.

Failure Mode

The majority of tests were controlled through post-failure and into residual strength. Residual strength values were not obtained for the majority of tests. The specimen jackets ruptured due to excessive specimen dilation. The subsequent intrusion of the specimens by confining fluid invalidated the residual strength results. Specimens G25 and D27 were tested successfully through to residual values by reconfiguring the jacketing procedure. The specimens in general exhibited Class II post-peak failure characteristics.

Strength Envelopes

The peak strength envelopes including two residual strength envelopes of the specimens are given in Appendix A. These envelopes are based on the empirical failure criterion of rocks, established by Hoek and Brown (10).

The derived material constant values of m and s and m_r and s_r, corresponding to the peak and residual strength envelopes, respectively, are given for each specimen in the relevant graph of Appendix A.

5. DISCUSSION

Specimen Jacketing

Teflon jacketing material yielded plastically during extreme specimen dilation. Once yielded, the teflon sheared at the wire clamps located on the platen surfaces. This resulted in confining fluid intruding into the specimen. In subsequent tests, the teflon jackets were overlayed with bicycle inner tubing bands at the teflon/platen contacts. The wire clamps were replaced by O-rings. The bicycle tubing and the O-rings have the elasticity required to accommodate the extreme specimen dilation experienced during post-failure testing.

Triaxial Seal

Assembling of the triaxial chamber requires that the upper chamber be lowered onto the base. The base houses the main seals. Lowering of the upper chamber over the seals, caused damage to the main seal and resulted in confinement fluid pressure loss during triaxial tests. The seal will require redesign.

Computer Software

Software, written in-house, to control the multi-stage test, was found to be satisfactory. Incorporated in software were servo-hydraulic loop stabilization times. Loop stabilization times allow the servo-hydraulics sufficient time to respond to a computer command. Sufficient response time allows the DC error of the servo-valve to stabilize at zero prior to further computer commands being initiated.

Material Constants

Material constants were determined by Hoek and Brown's method (10). For the specimens originating from Pinawa, Manitoba, the m values for intact rock are between 28 and 32. These results are in close agreement with the m values of 29 to 32 of the previous test

programs for the Pinawa rock, obtained by conventional triaxial test methods. Insufficient data are available from previous test programs for similar comparisons to be made with respect to the performance of Atikokan, Ontario and Lac St. Jean, Quebec specimens.

6. CONCLUSIONS

The MTS 815 Rock Mechanics Test System was used successfully for this test program. The servo-hydraulic system under computer test control was able to achieve post-failure strength determinations of the specimens. The number of successful tests increased as specimen jacketing and software modifications were made during the test program.

The determined values of Young's modulus, uniaxial compressive strength, and m and s material constants, were in agreement with values determined in other test programs. Previous test programs were performed using a Tinius Olsen test system under manual control. The Tinius Olsen test system lacks the servo-hydraulic controls required to undertake post-failure tests.

In the next step of testing technology development the MTS test system will be used to undertake a post-failure uniaxial test program. Hard rock specimens exhibiting Class II failure characteristics will be used in this test program. The tests are to be conducted by using the control mode described by Okubo and Nishimatsu (11). This control mode is based on a linear combination of stress and strain, where the feedback signal is continuously monitored. The program signal is continuously adjusted through use of software. Preliminary test runs indicate that it is a viable alternative for post-failure uniaxial tests over that described by Gorski (5). The test program will be undertaken in May, 1987.

7. REFERENCES

1. Wawersik, W.R. "A study of brittle rock fracture in laboratory compression experiments"; *Int J Rock Mech Min Sci* 7; 560-575; 1970.

2. Gyenge, M. "Laboratory test requirements for post failure strength properties of rocks"; *Division Report* $MRP/MRL82-33(TR)$; CANMET, Energy, Mines, and Resources Canada; 1982.

3. Gorski, B. "The design and operation of a stiff triaxial assembly for post-failure rock property testing"; *Division Report* $MRP/MRL82-81(TR)$; CANMET, Energy, Mines and Resources Canada; 1982.

4. Gorski, B. "The design and operation of a parallel stiff compression apparatus"; *Division Report* $MRP/MRL84-36(TR)$; CANMET, Energy, Mines and Resources Canada; 1984.

5. Gorski, B. "Post-Failure uniaxial strength determinations using a servo-hydraulic test system"; *Division Report* $MRL87-33(INT)$; CANMET, Energy, Mines and Resources Canada; 1987.

6. Kovari, K. and Tisa, A. "Multiple failure state and strain controlled triaxial tests"; *Rock Mechanics* 7: 17-33; 1975.

7. Jackson, R. "Summary of mechanical properties of Lac Du Bonnet and Eye-Dashwa specimens"; *Division Report* $MRP/MRL84-85(TR)$; CANMET, Energy, Mines and Resources Canada; 1984.

8. Shimotani, T. "Evaluation of testing procedures for minimizing rock sample requirement"; *Division Report* $MRP/MRL83-19(TR)$; CANMET, Energy, Mines and Resources Canada; 1983.

9. Gyenge, M. and Herget, G. "Pit slope Manual 3-2; Laboratory tests for design parameters"; *CANMET Report* $77-26$; CANMET, Energy, Mines and Resources Canada; 1977.

10. Hoek, E. and Brown, E.T. *Underground excavations in rock*; Institute of Mining and Metallurgy; 527pp.; 1980.

11. Okubo, S. and Nishimatsu, Y. "Uniaxial compression testing using a linear combination of stress and strain as the control variable"; *Int J Rock Mech Min Sci and Geomech, Abstr.*; 22:5:323-330; 1985.

Table 1 - Specimen selection data

Specimen Number	Depth Interval	Bore Hole	Rock Type	Length (mm)	Diameter (mm)	δ (g/cm^3)
G19	1050.5	ATK5	Granite	89.40	44.72	2.63
G20	1000.5	URL2	Granite	91.40	45.00	2.63
G21	98.2	WN2	Granite	91.68	44.70	2.62
G22	534.0	ATK5	Granite	91.50	44.70	2.62
G23	156.6	URL5	Granite	90.00	44.82	2.62
G24	810.2	ATK5	Granite	90.20	45.14	2.61
G25	793.3	URL2	Granite	89.50	45.26	2.63
D26	-	-	Diabase	89.92	44.00	2.94
D27	-	-	Diabase	88.90	44.00	2.94

Table 2 - Multi-stage triaxial test results

Compressive strength			σ_3=6.9 MPa		σ_3=13.8 MPa		σ_3=20.7 MPa		σ_3=27.6 MPa		σ_3=34.5 MPa		Modulus
Specimen Number	Q_u (MPa)	ε_{peak} (%)	σ_1 (MPa)	ε_{peak} (%)	σ_1 (MPa)	ε_{peak} (%)	σ_1 (MPa)	ε_{peak} (%)	σ_1 (MPa)	ε_{peak} (%)	σ_1 (MPa)	ε_{peak} (%)	E (GPa)
G19	140.2	0.29	230.5	0.48	316.7	0.66	377.1	0.78	466.1	1.02	-	-	50.7
G20	124.2	0.37	221.9	0.59	305.8	0.79	349.8	0.88	405.3	1.02	474.8	1.25	44.3
G21	97.5	0.16	290.1	0.51	378.4	0.67	446.2	0.80	509.2	0.93	553.4	1.02	69.2
G22	114.0	0.19	231.9	0.42	296.9	0.54	358.4	0.66	-	-	-	-	47.4
G23	126.2	0.18	254.1	0.41	353.6	0.62	431.6	0.80	485.7	0.92	533.9	1.04	66.0
G24	85.3	0.16	183.2	0.40	237.0	0.52	283.3	0.61	324.5	0.70	409.3	0.91	42.2
G25	121.7	0.29	221.9	0.48	306.9	0.67	363.4	0.80	403.9	0.88	478.1	1.12	49.9
D26	297.7	0.38	353.6	0.48	388.7	0.54	417.7	0.59	445.8	0.64	528.4	0.86	77.0
D27	194.1	0.24	341.5	0.49	386.5	0.57	435.5	0.67	466.7	0.73	531.0	0.95	80.4

APPENDIX A

STRENGTH ENVELOPES

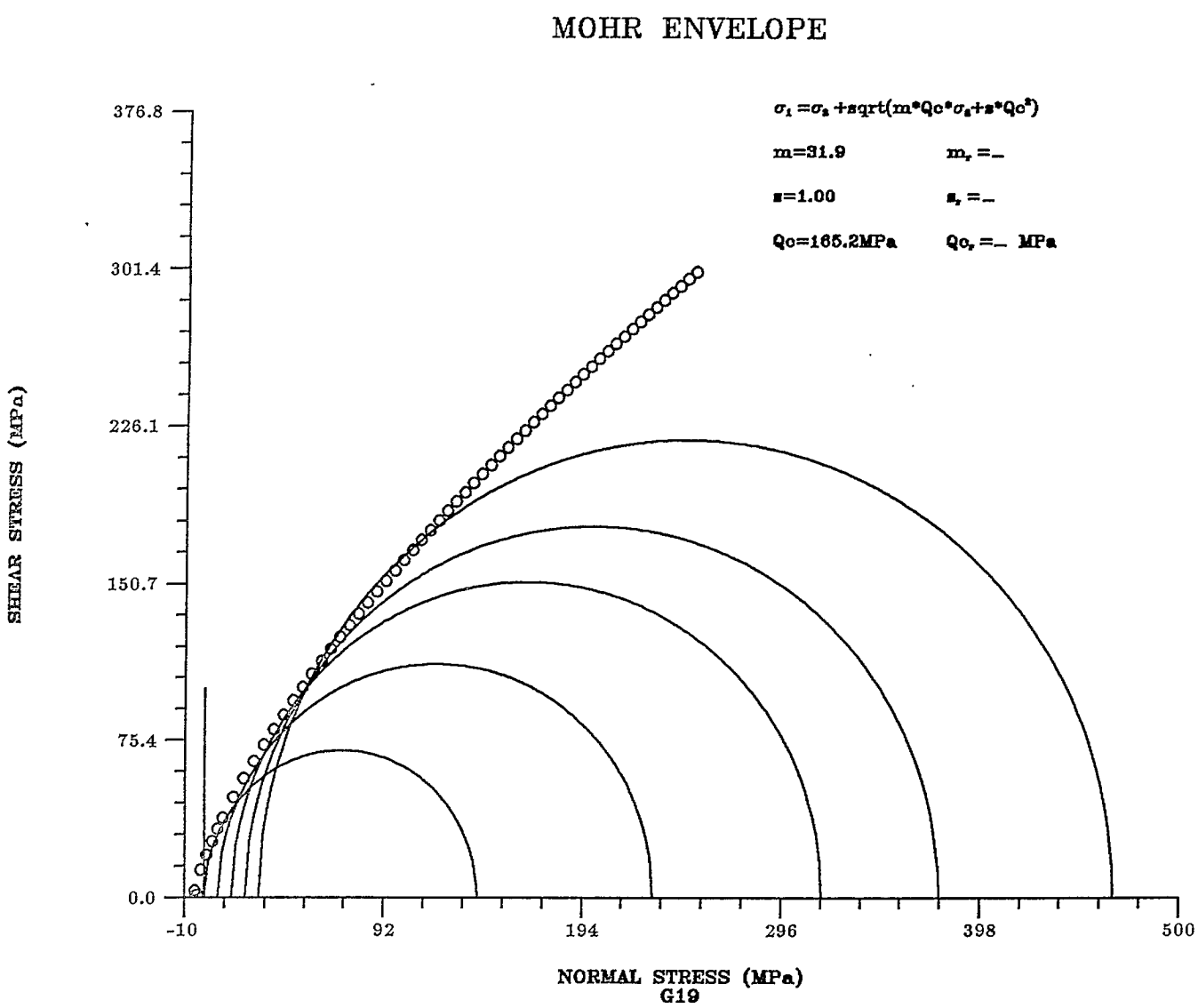

Fig. A - 1 Specimen G19

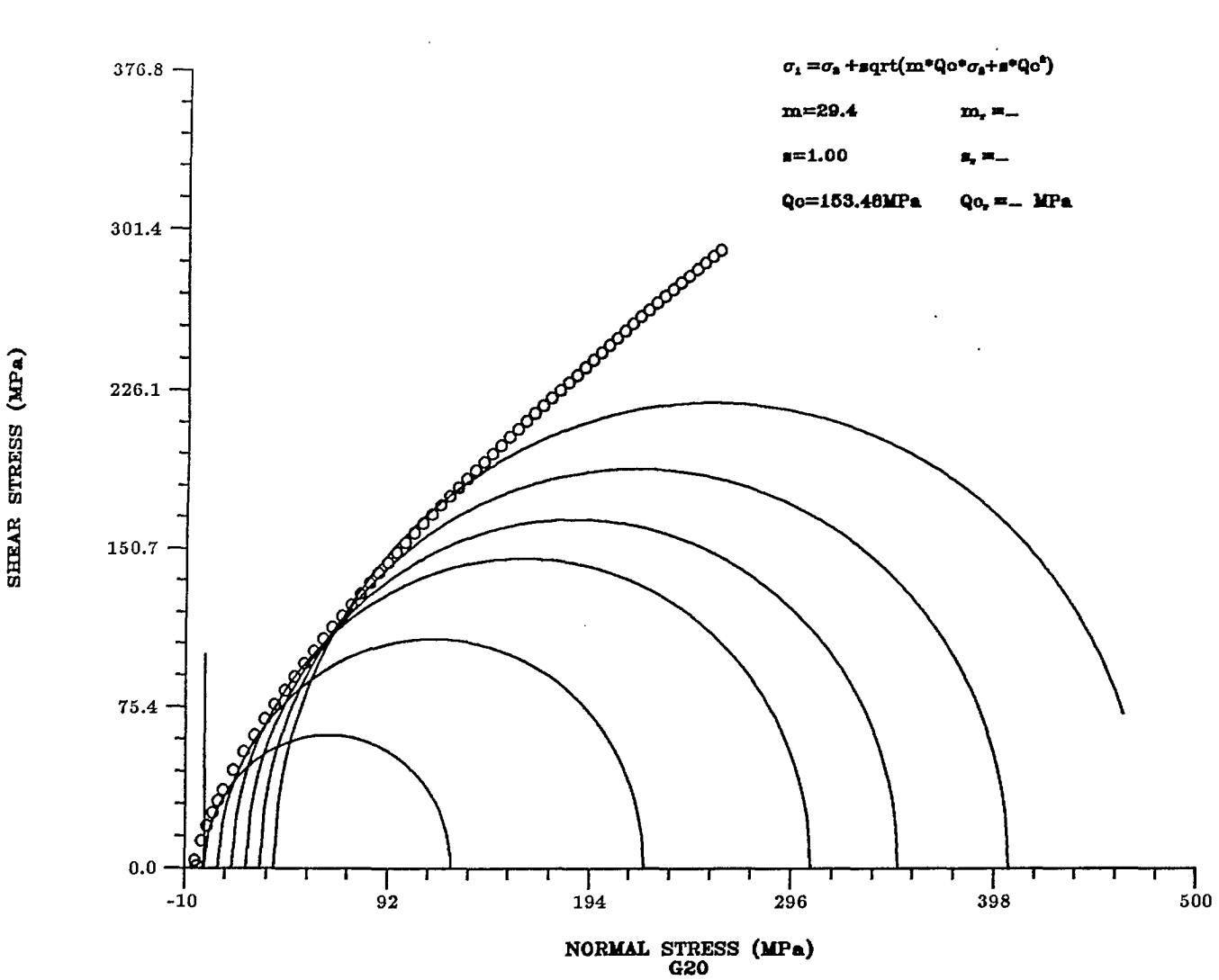

Fig. A - 2 Specimen G20

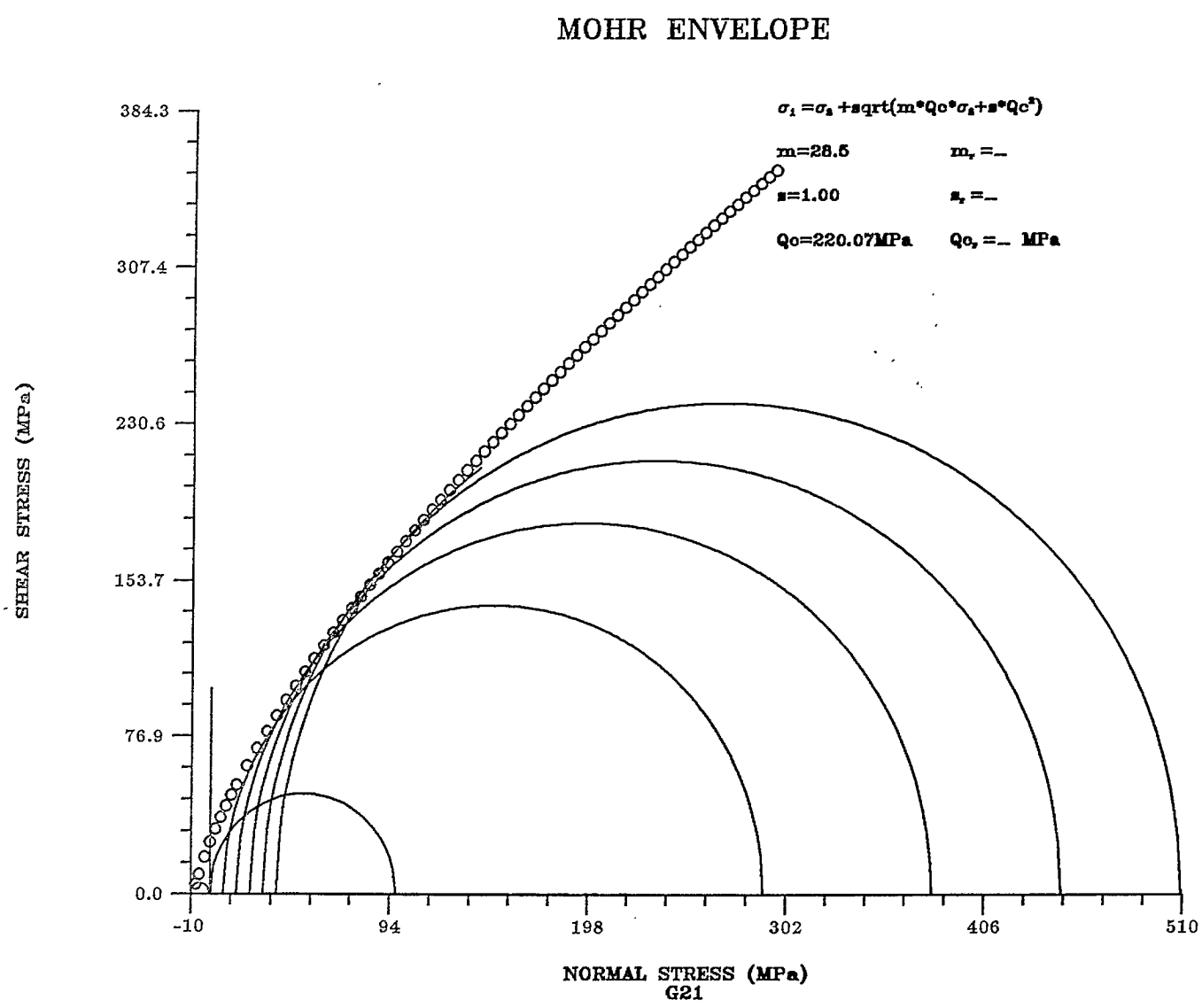

Fig. A - 3 Specimen G21

MOHR ENVELOPE

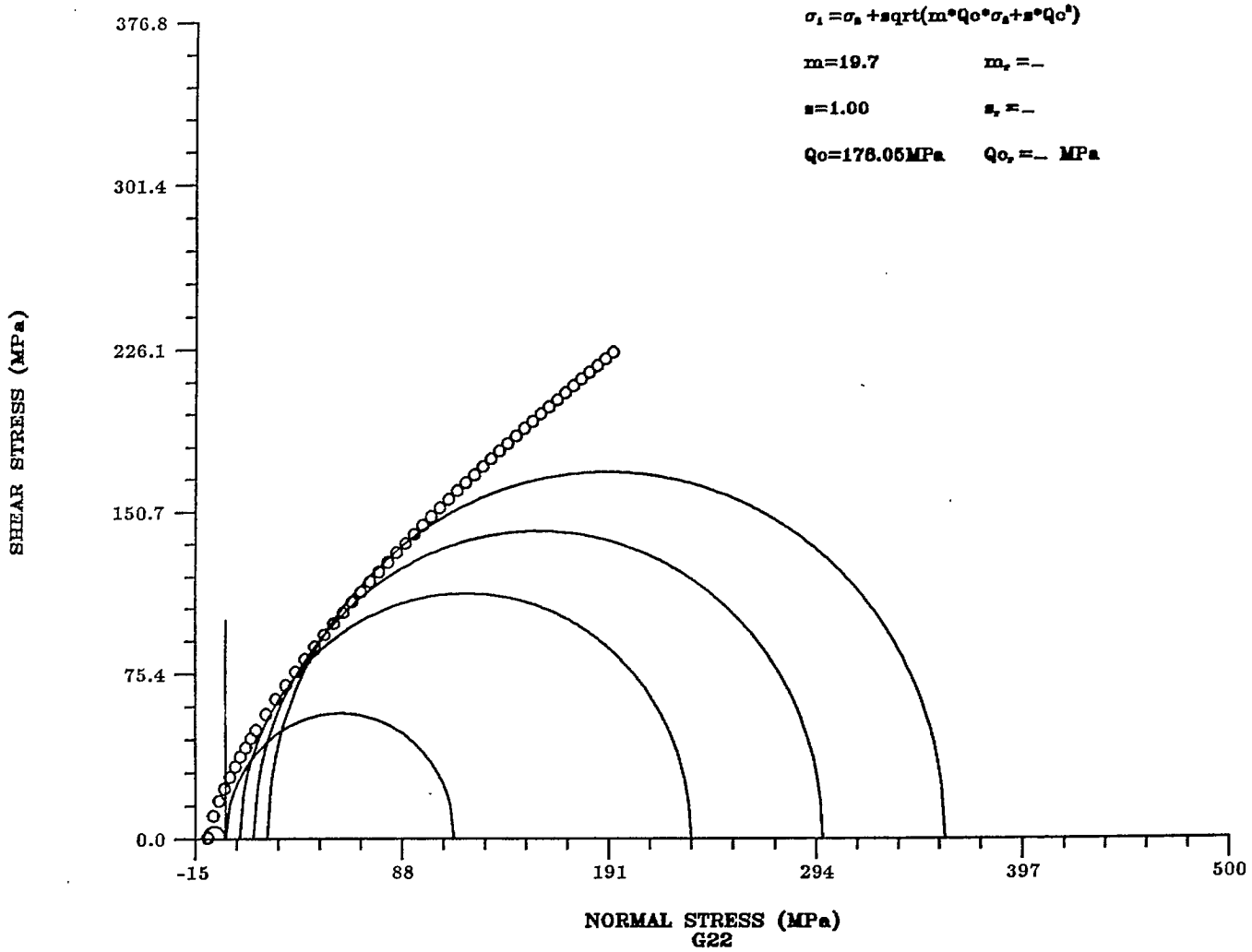

Fig. A - 4 Specimen G22

MOHR ENVELOPE

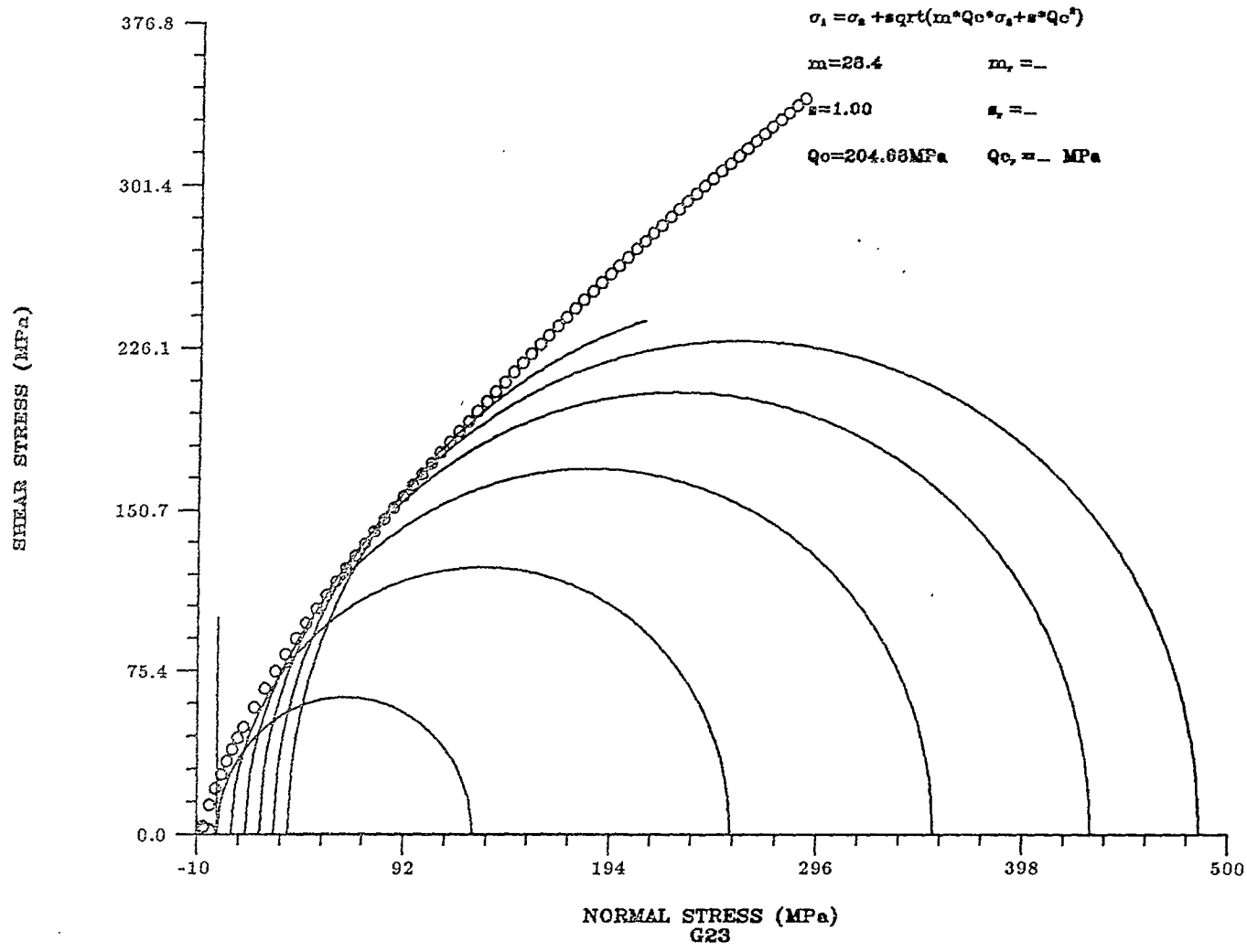

Fig. A - 5 Specimen G23

MOHR ENVELOPE

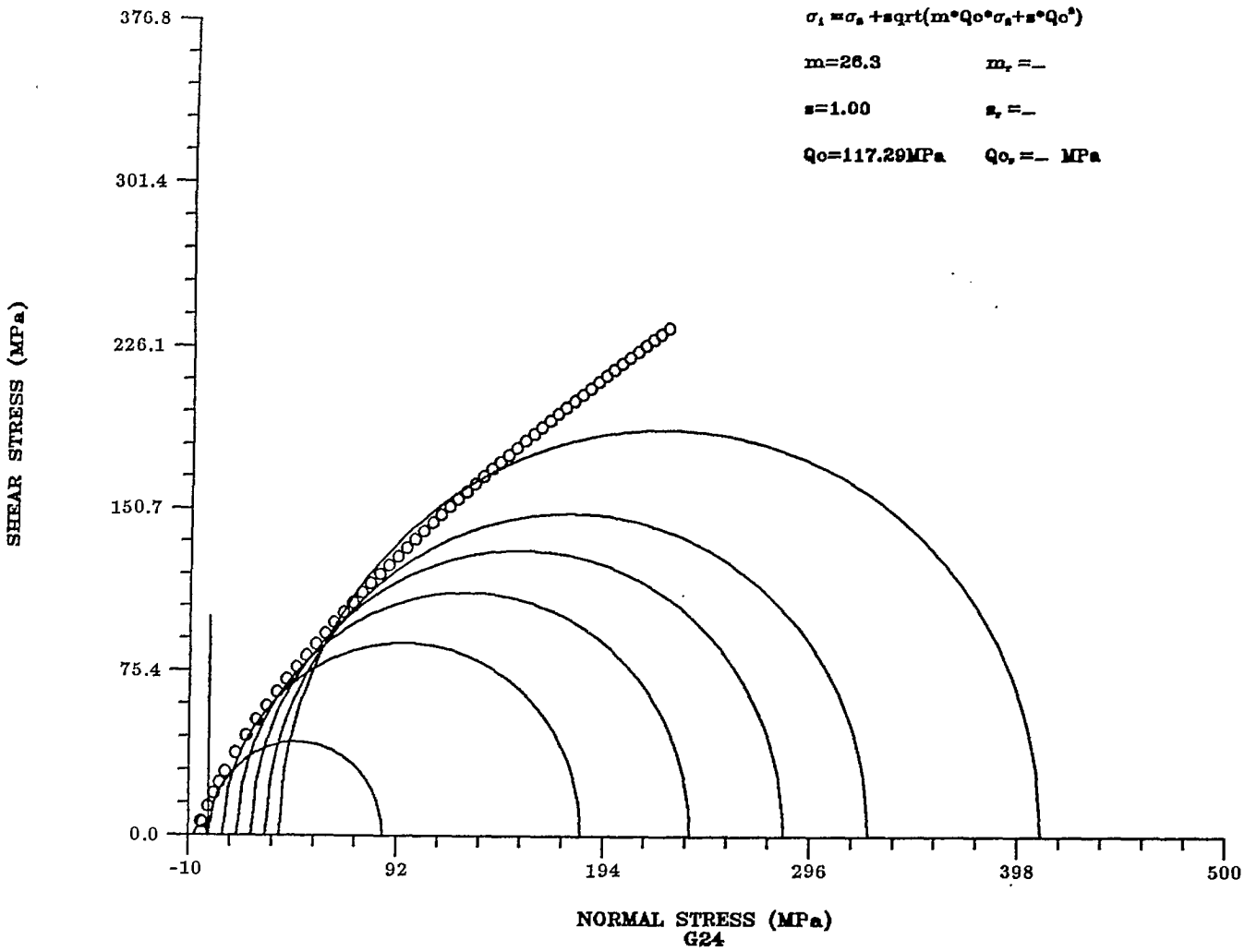

Fig. A - 6 Specimen G24

MOHR ENVELOPE

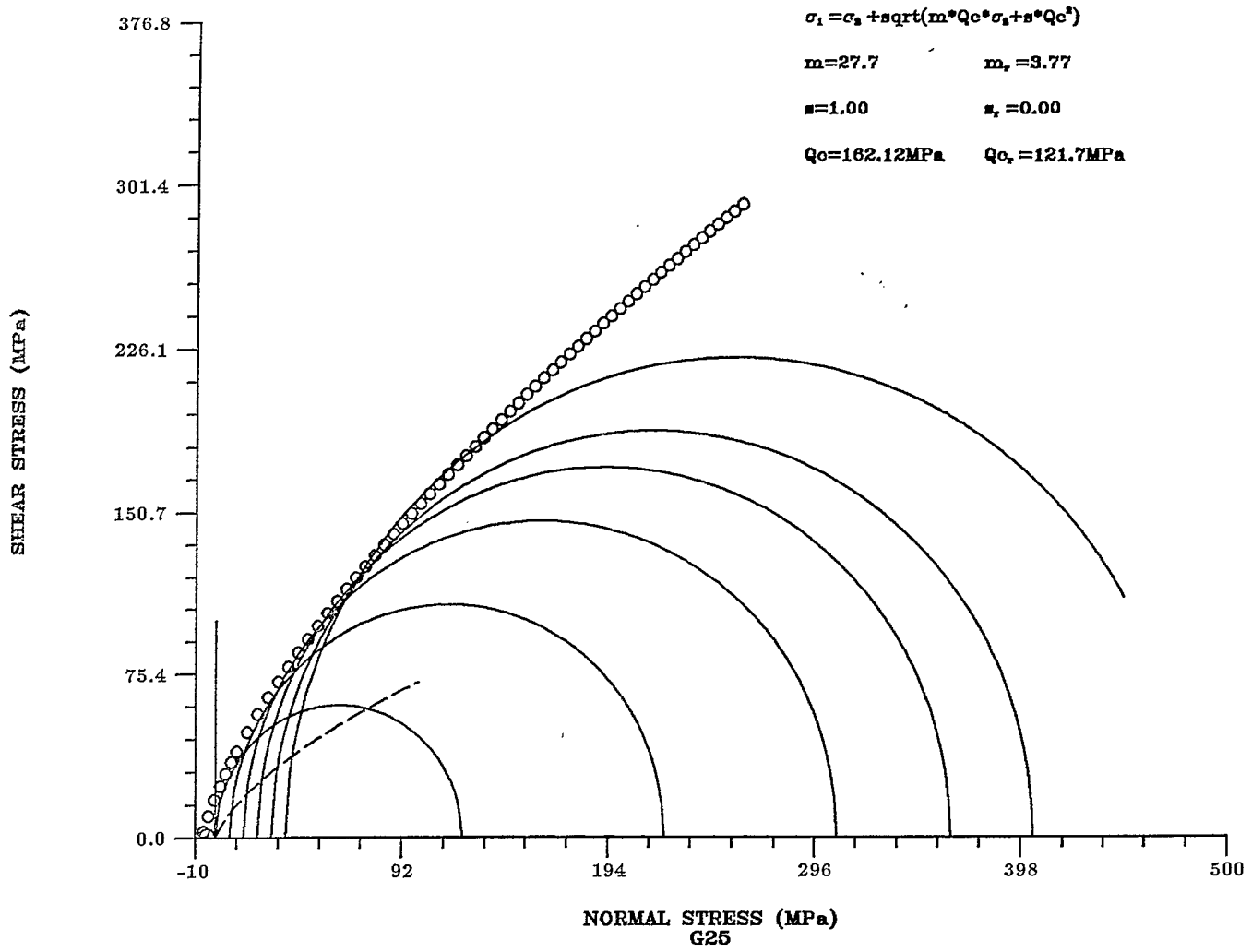

Fig. A - 7 Specimen G25

MOHR ENVELOPE

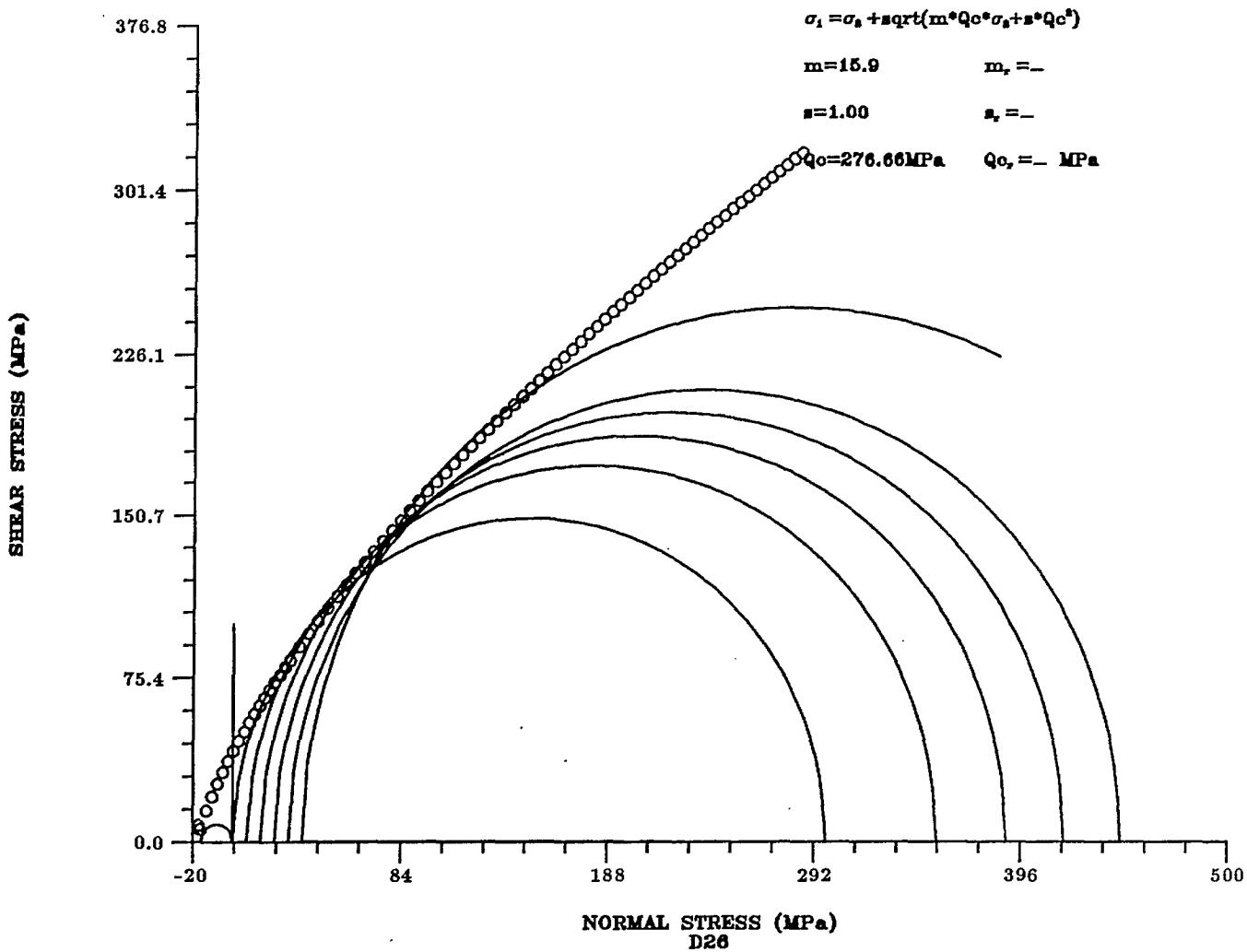

Fig. A - 8 Specimen D26

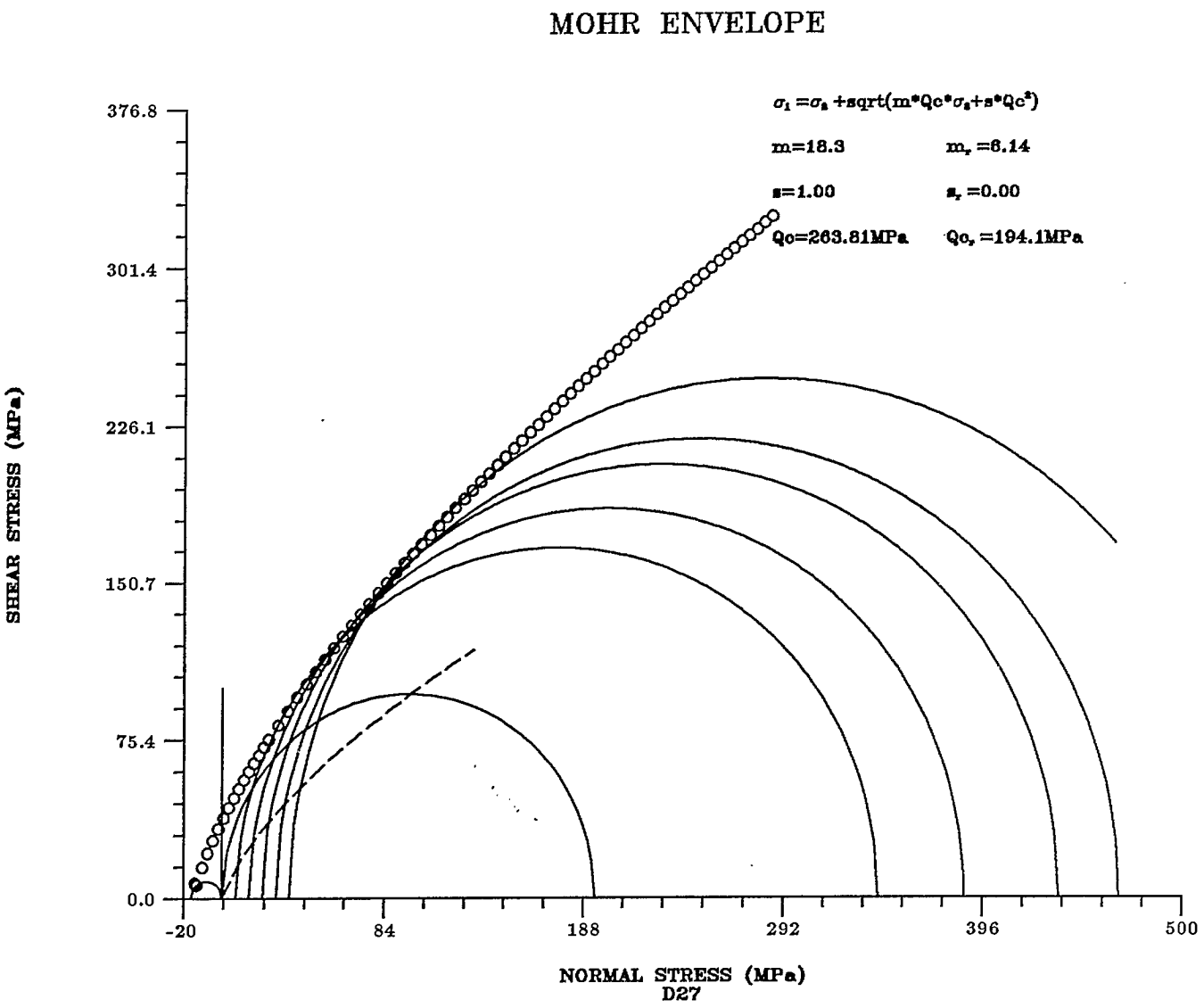

Fig. A - 9 Specimen D27

APPENDIX B

STRESS-STRAIN RESULTS OF TESTS USING AXIAL LVDT No. 1

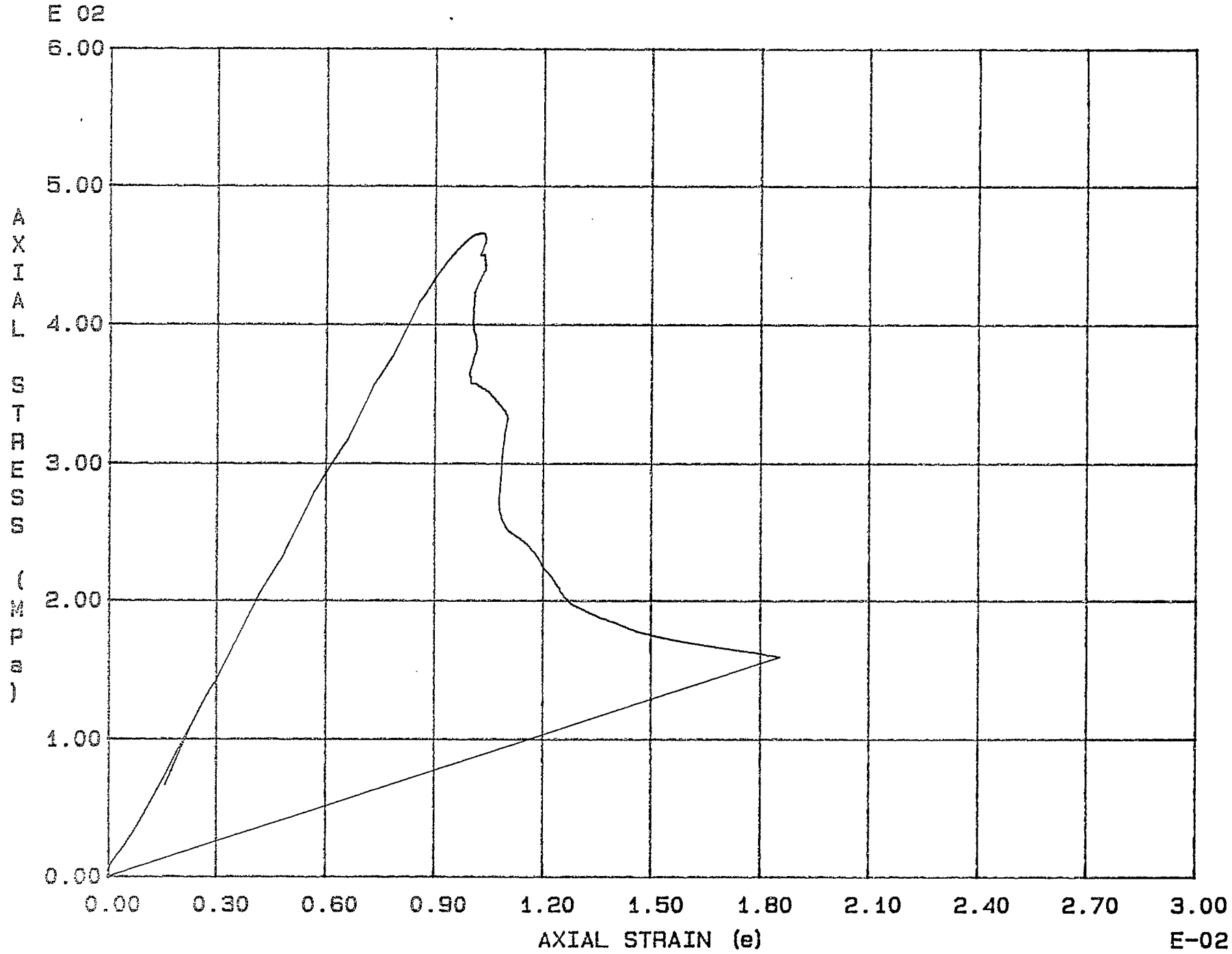

Fig. B - 1 Specimen G19

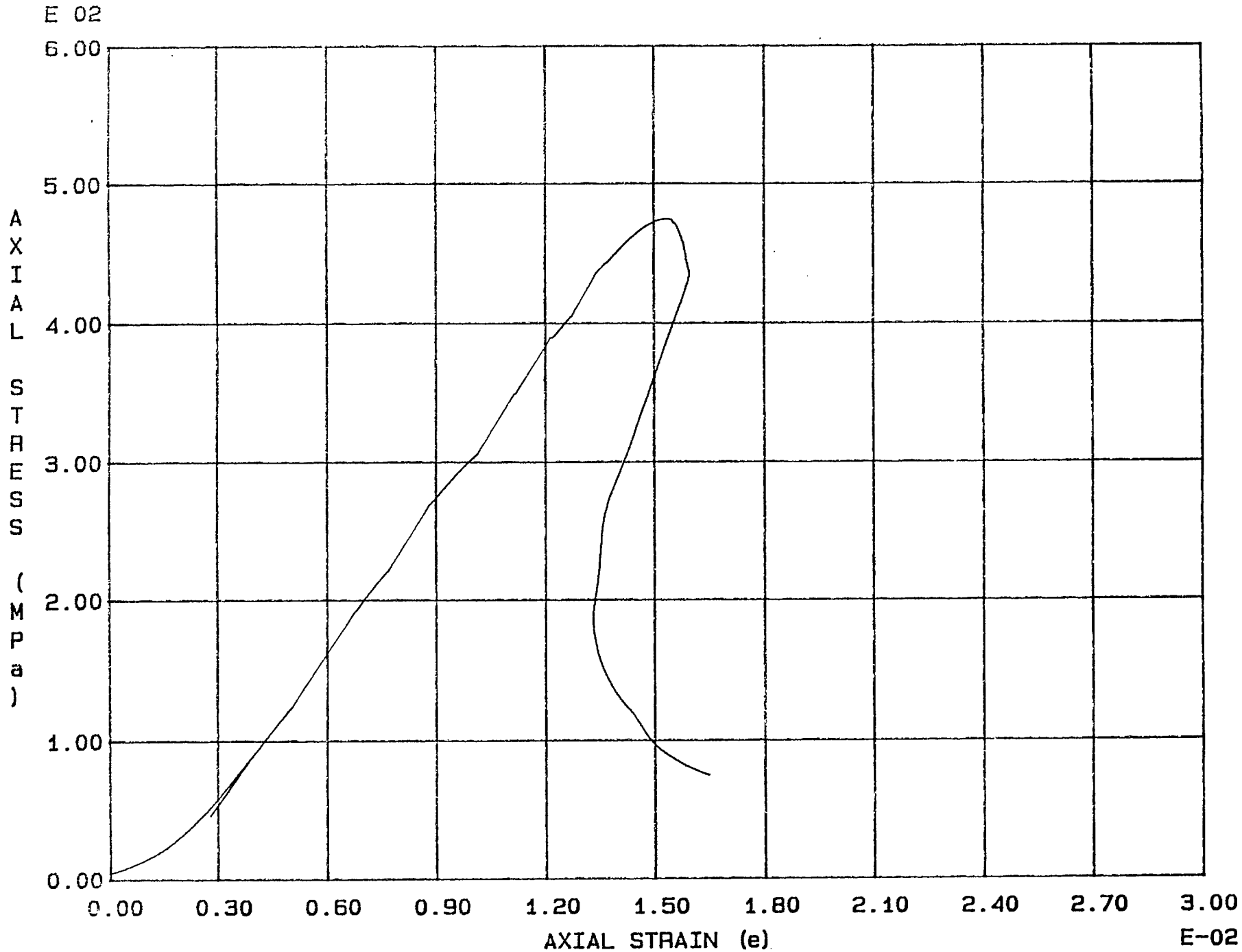

Fig. B - 2 Specimen G20

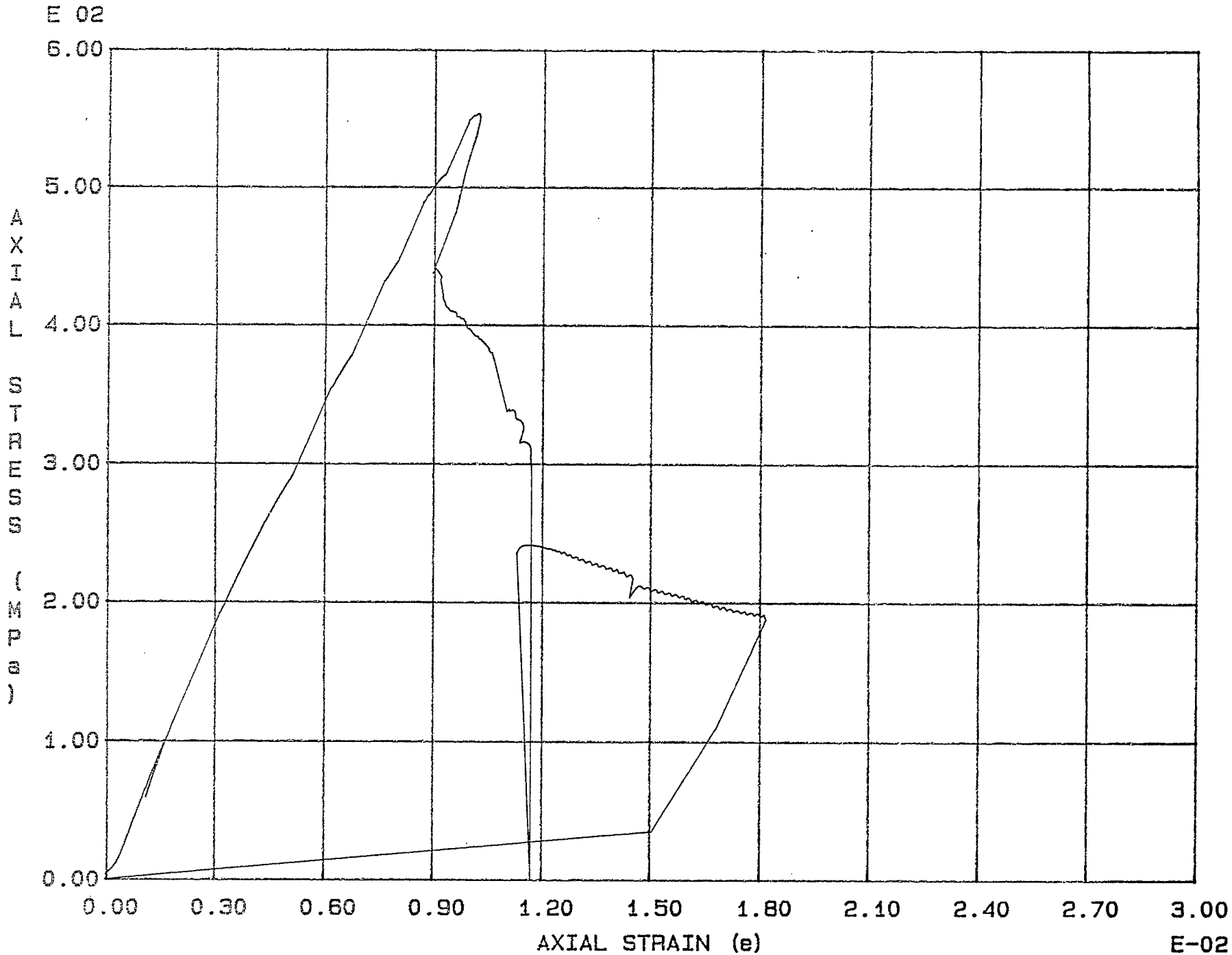

Fig. B - 3 Specimen G21

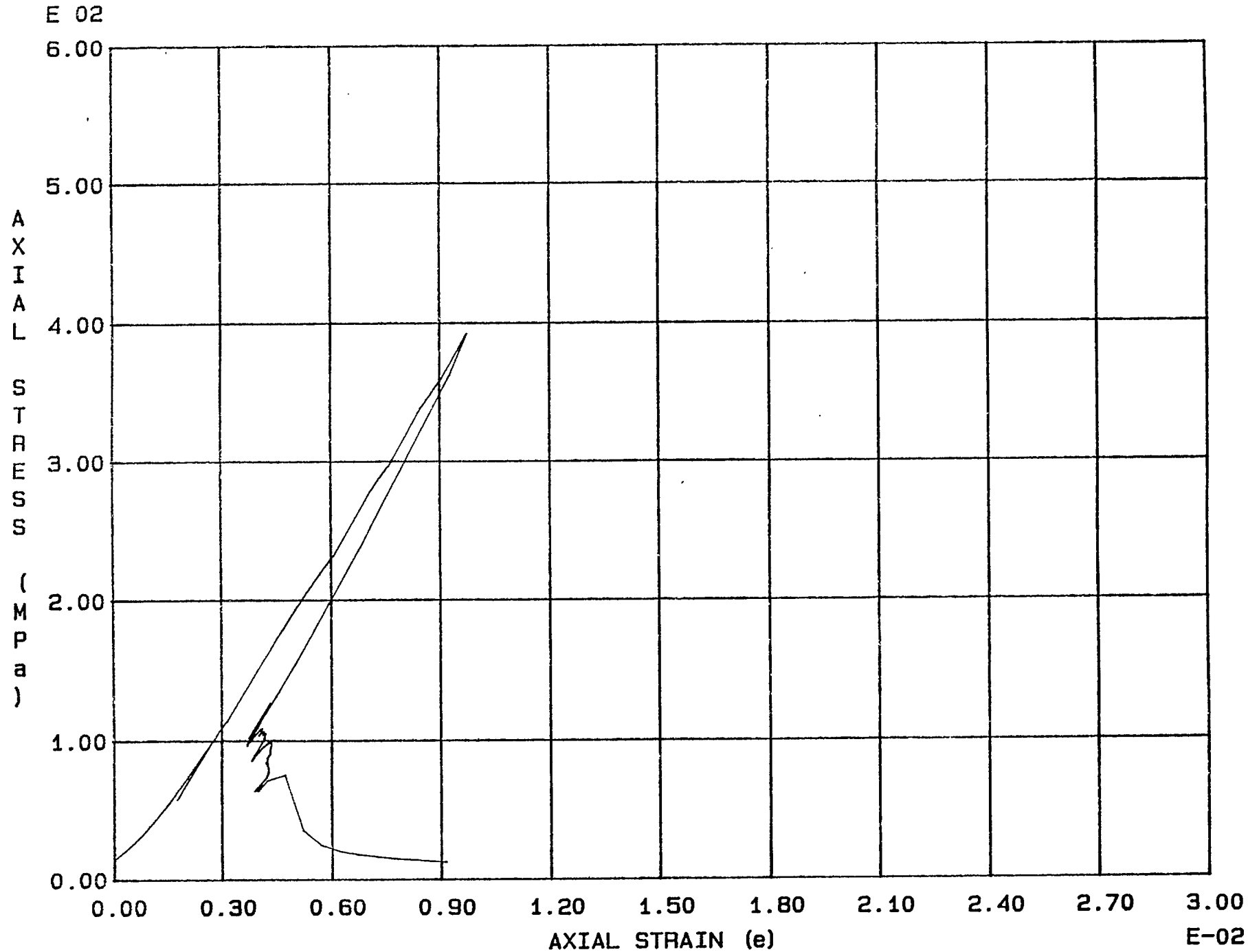

Fig. B - 4 Specimen G22

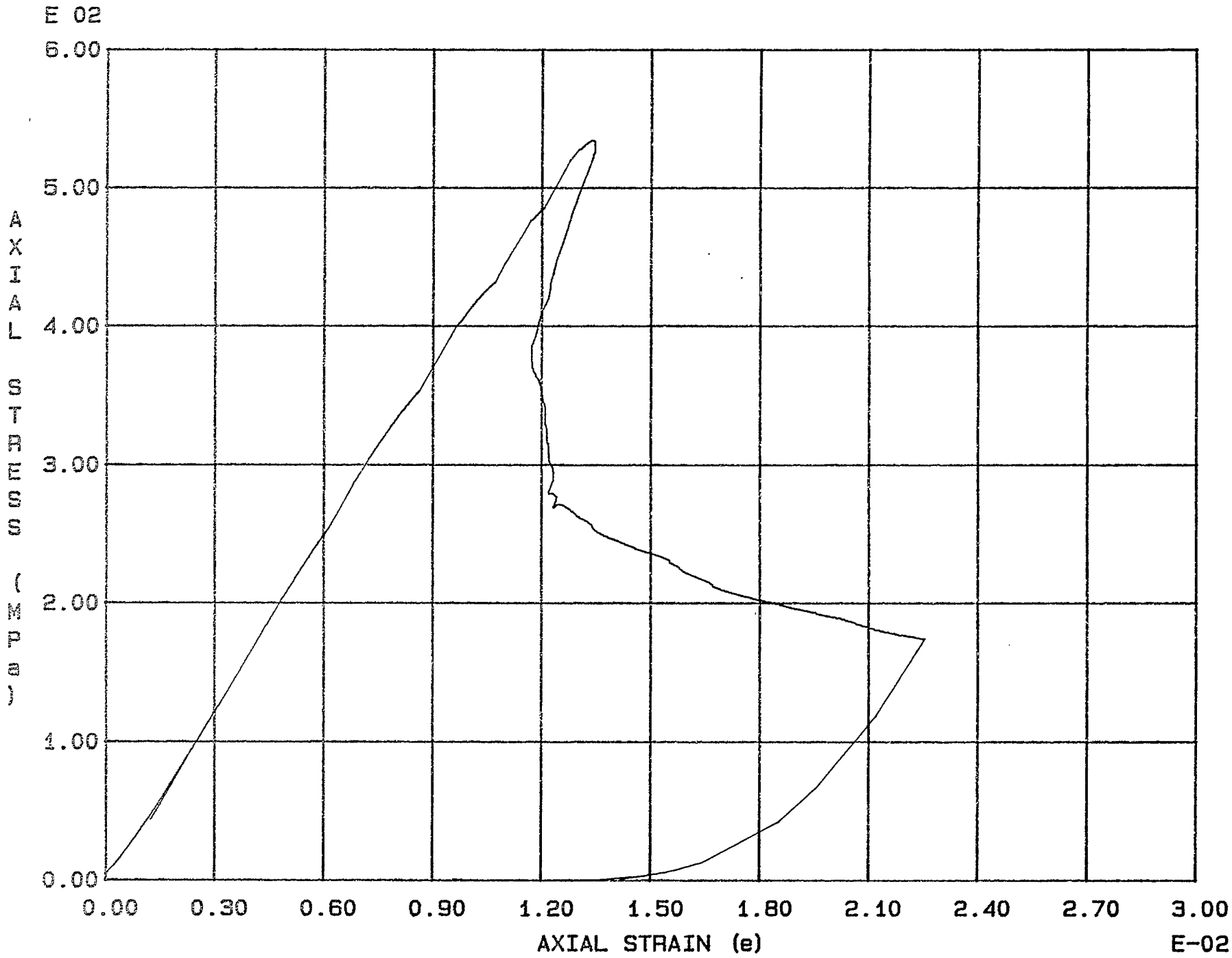

Fig. B - 5 Specimen G23

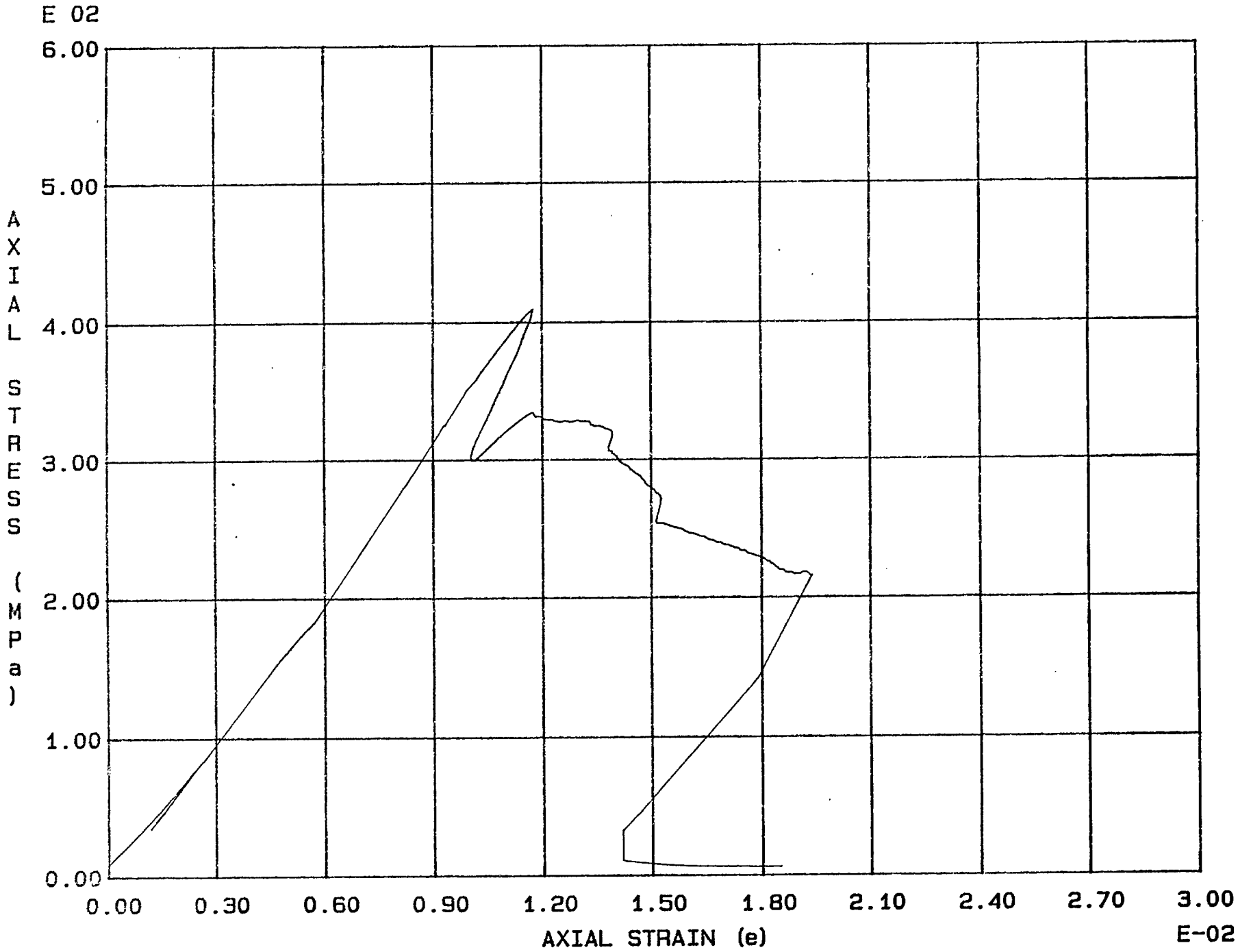

Fig. B - 6 Specimen G24

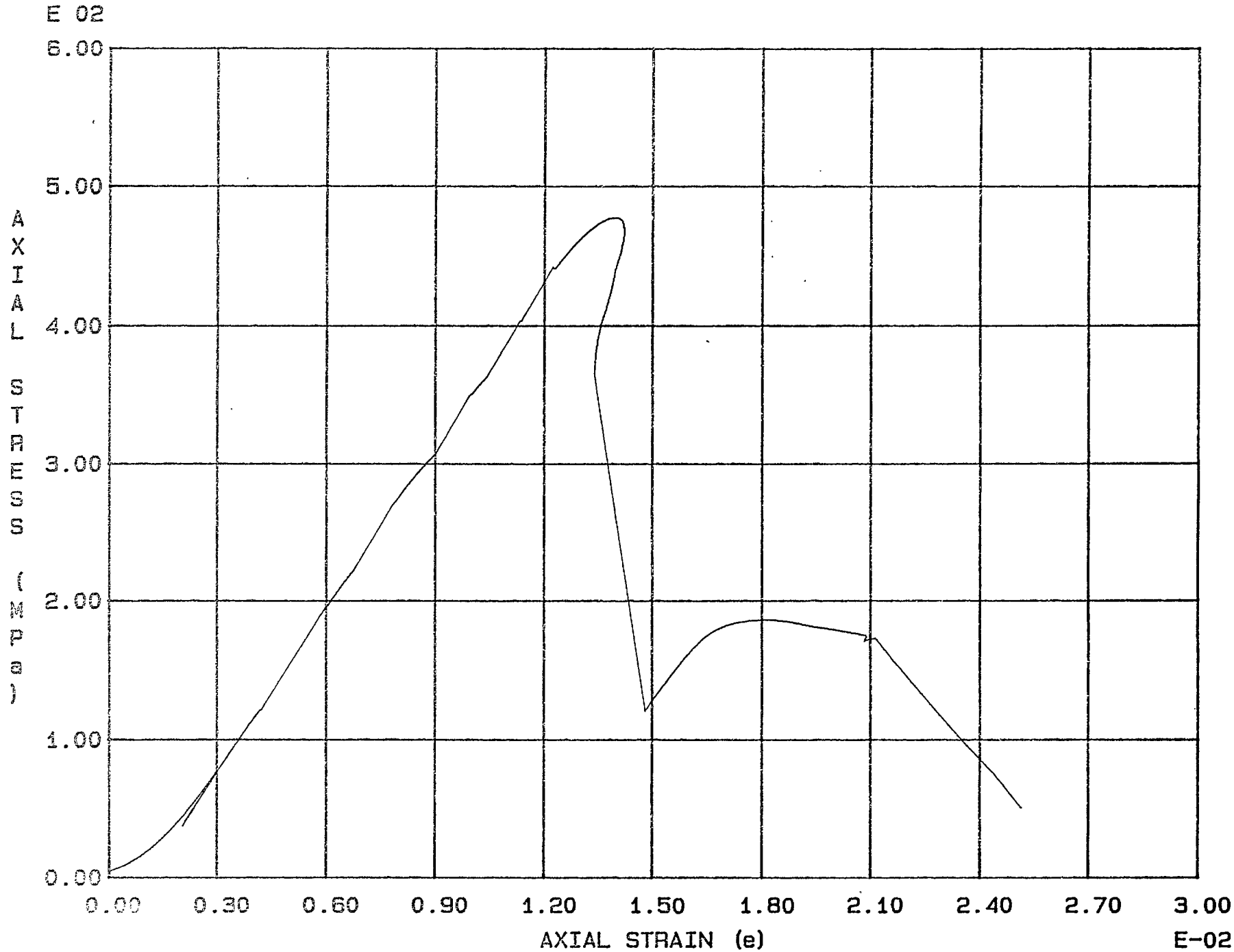

Fig. B - 7 Specimen G25

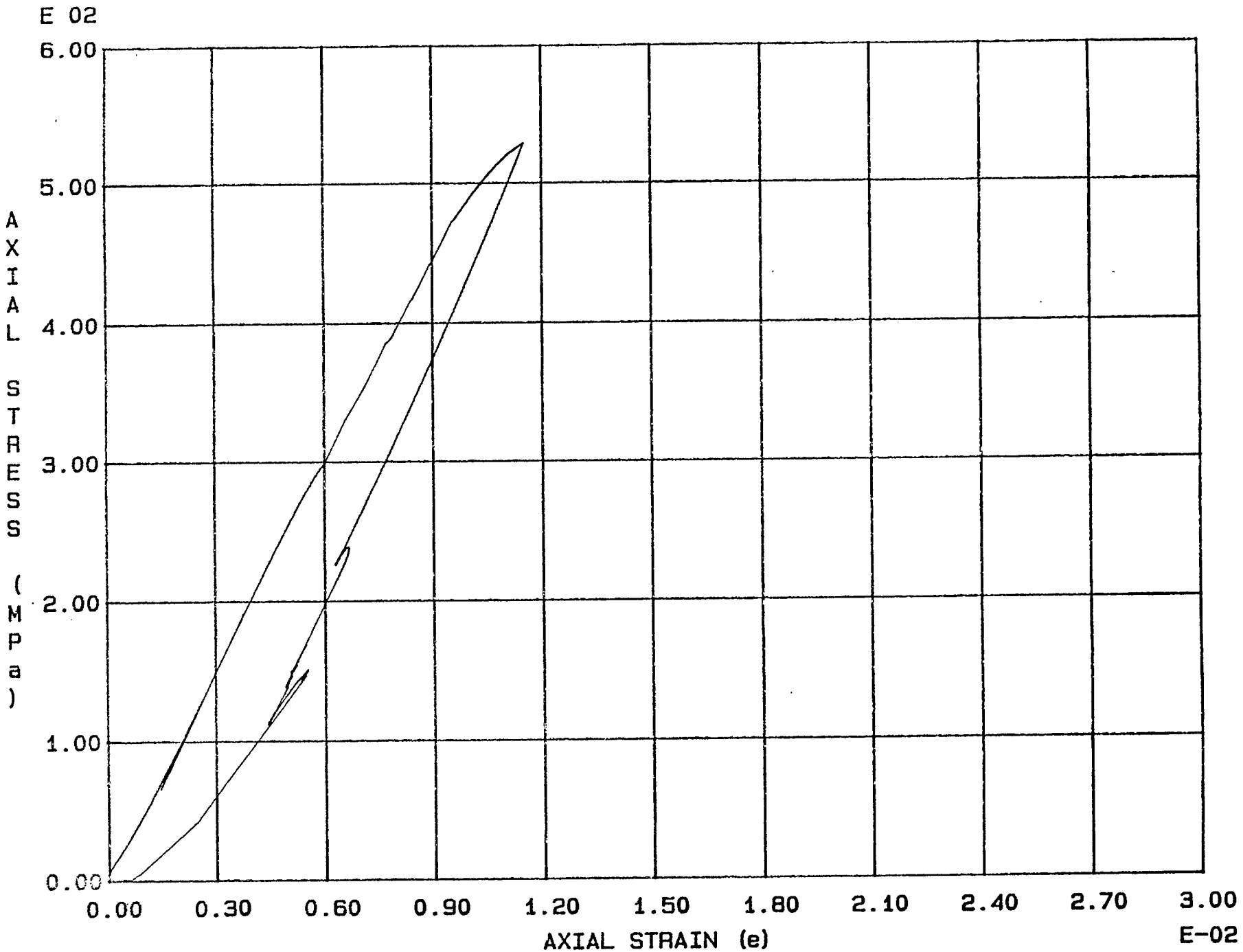

Fig. B - 8 Specimen D26

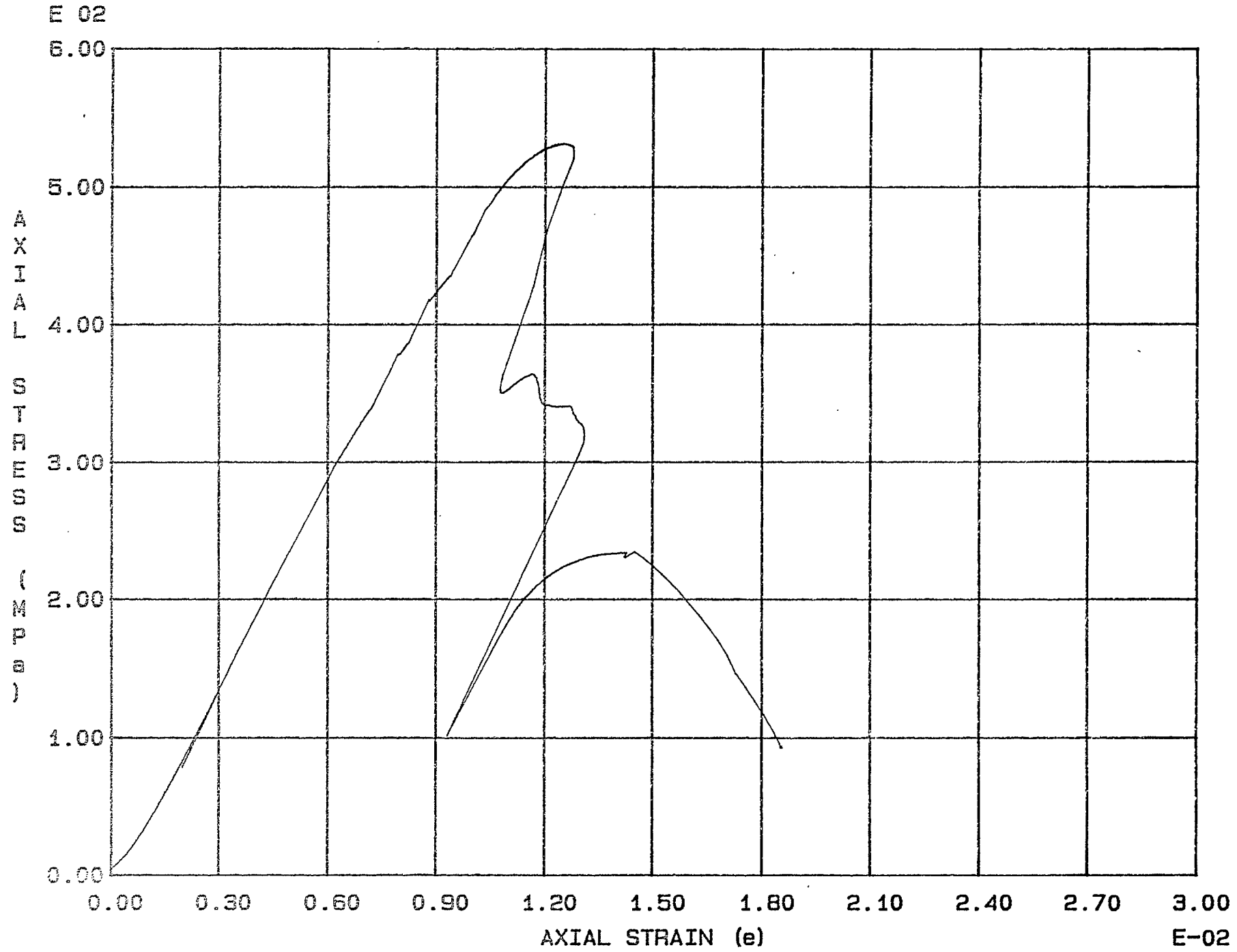

Fig. B - 9 Specimen D27

APPENDIX C

STRESS-STRAIN RESULTS OF TESTS USING CIRCUMFERENTIAL EXTENSOMETER

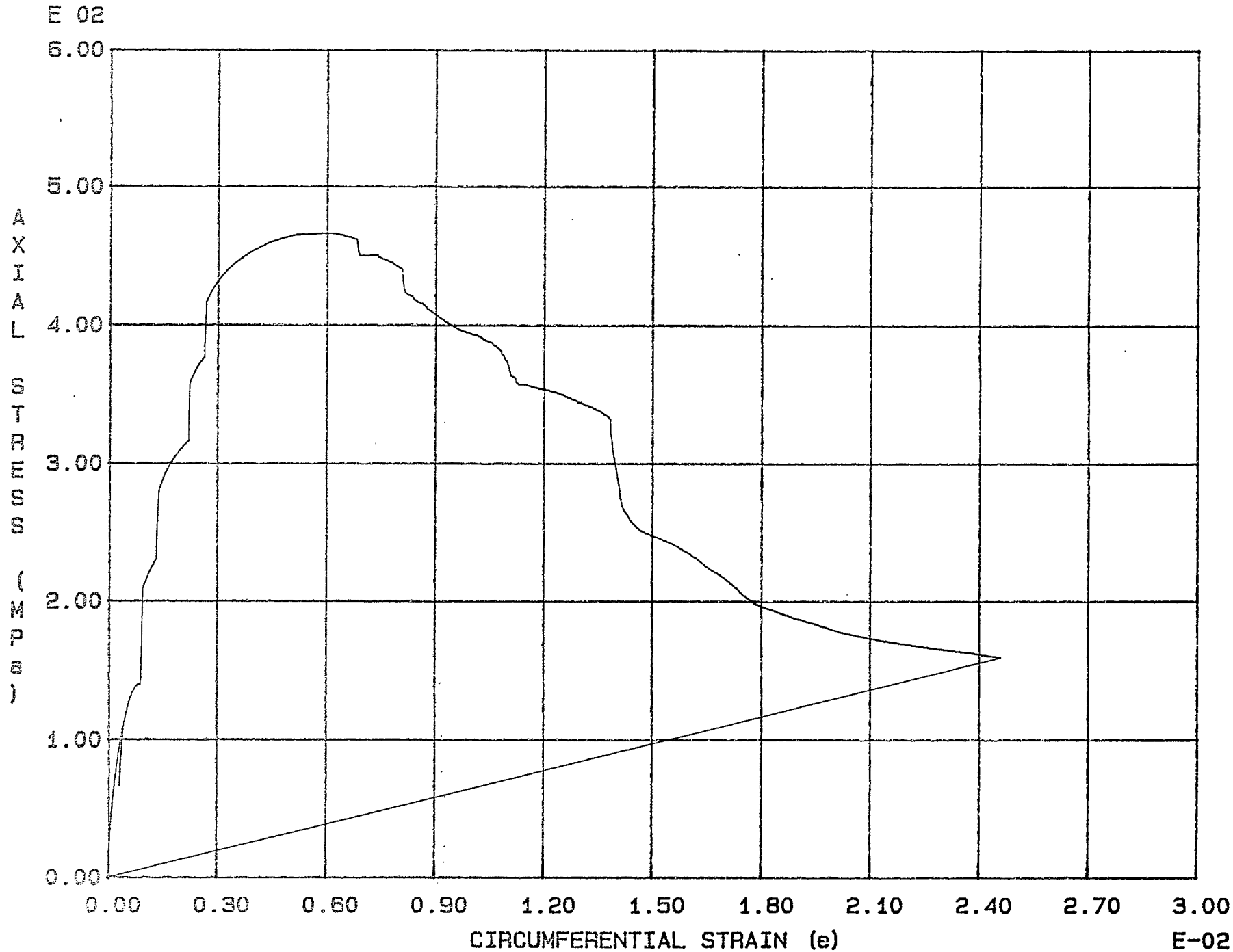

Fig. C - 1 Specimen G19

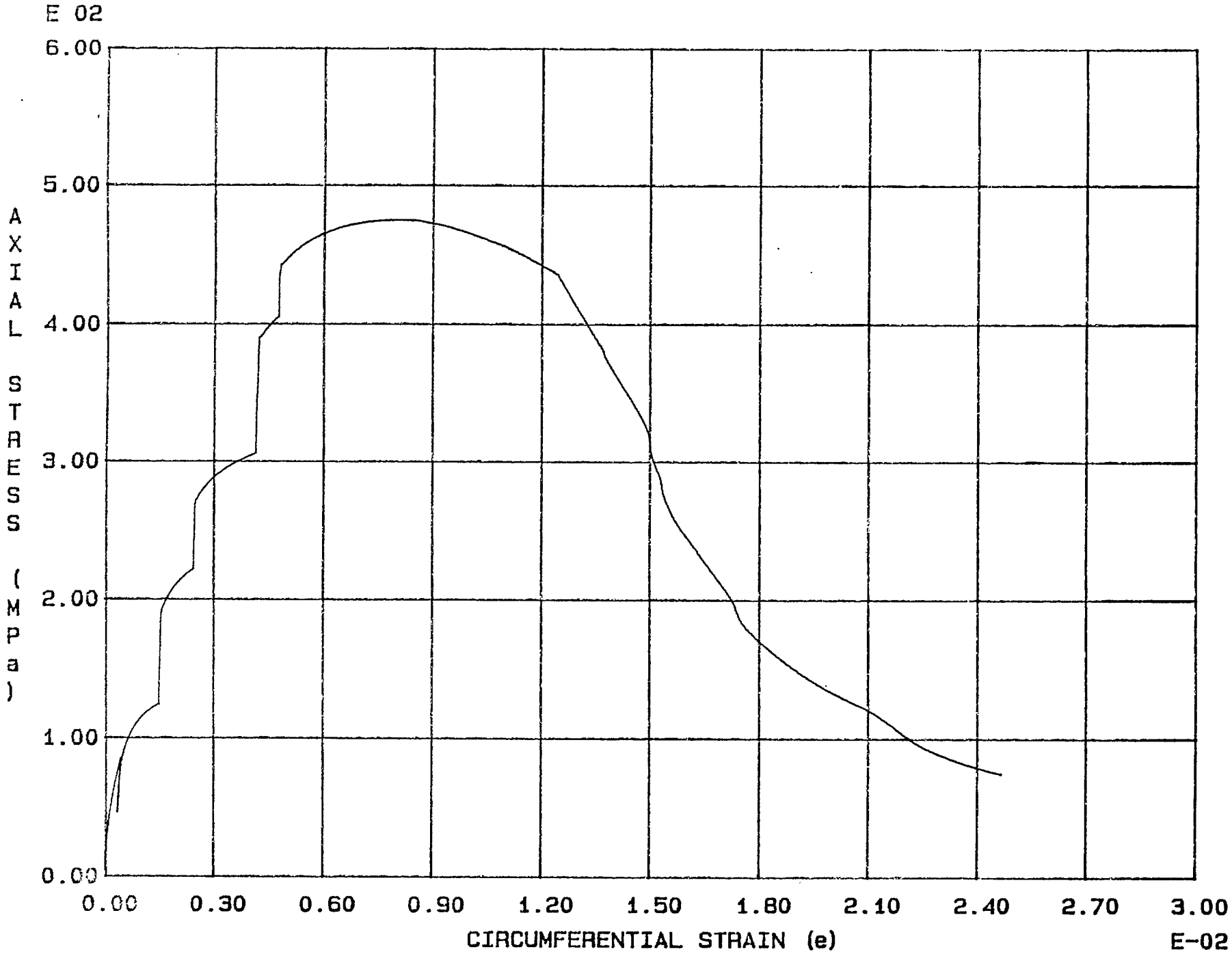

Fig. C - 2 Specimen G20

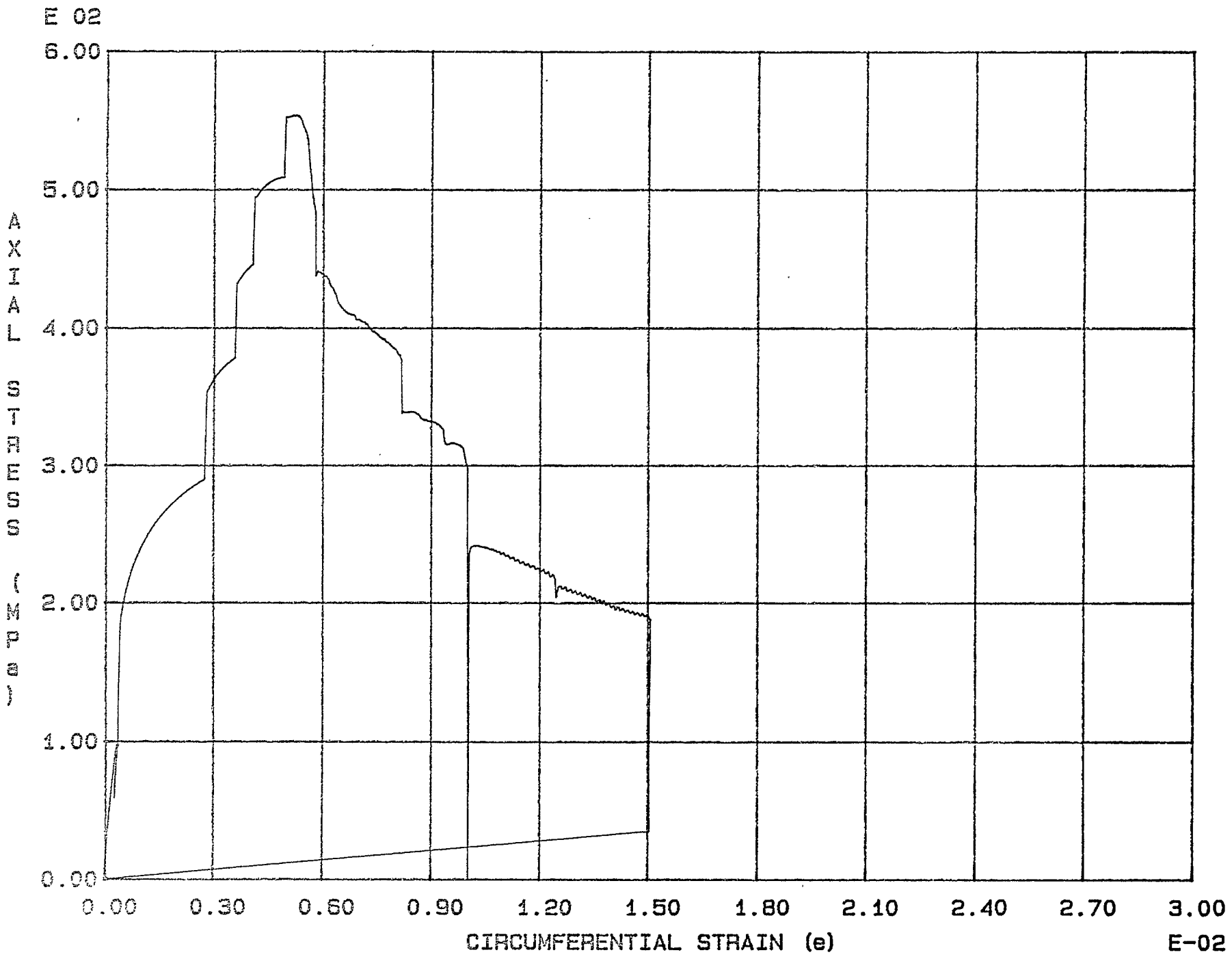

Fig. C - 3 Specimen G21

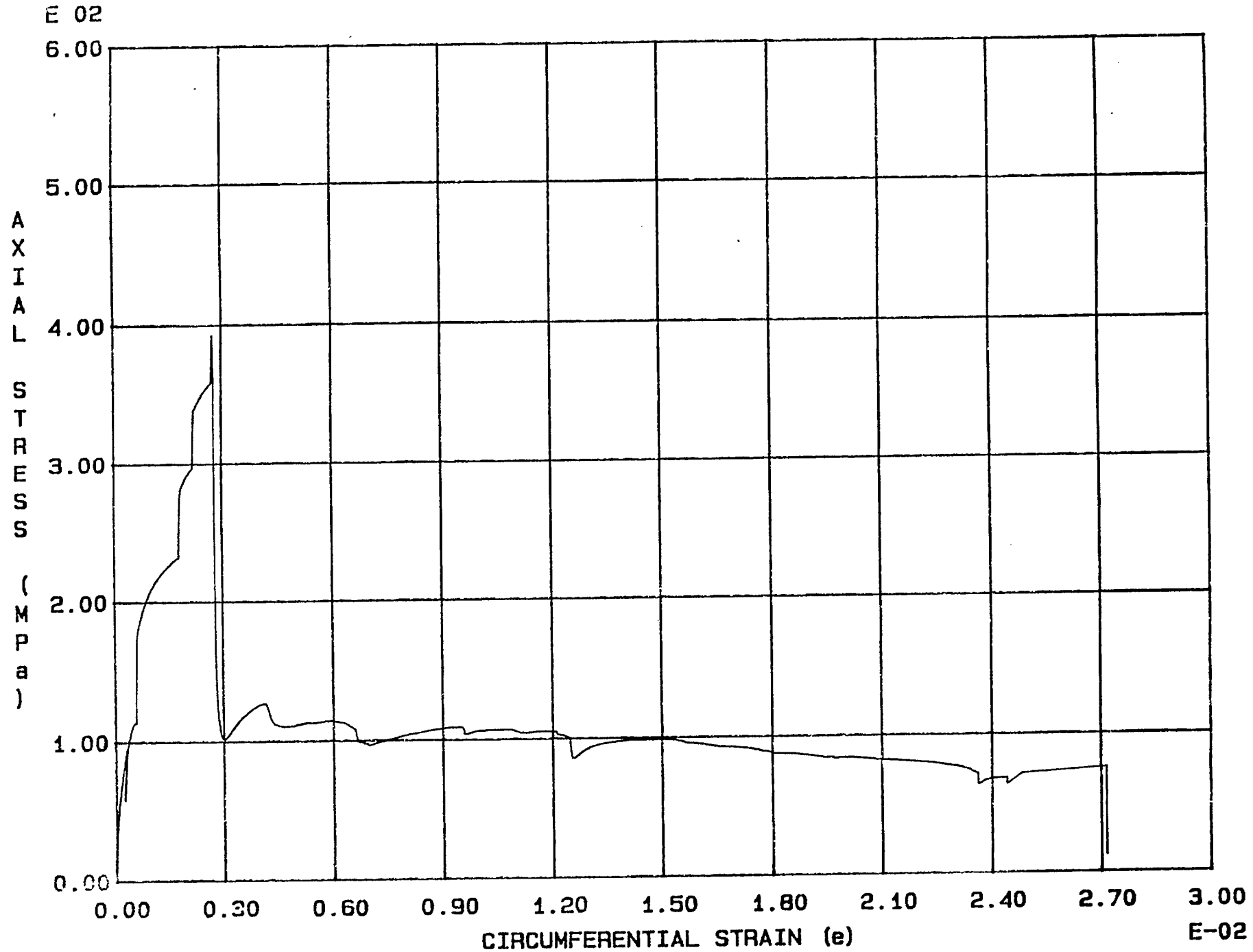

Fig. C - 4 Specimen G22

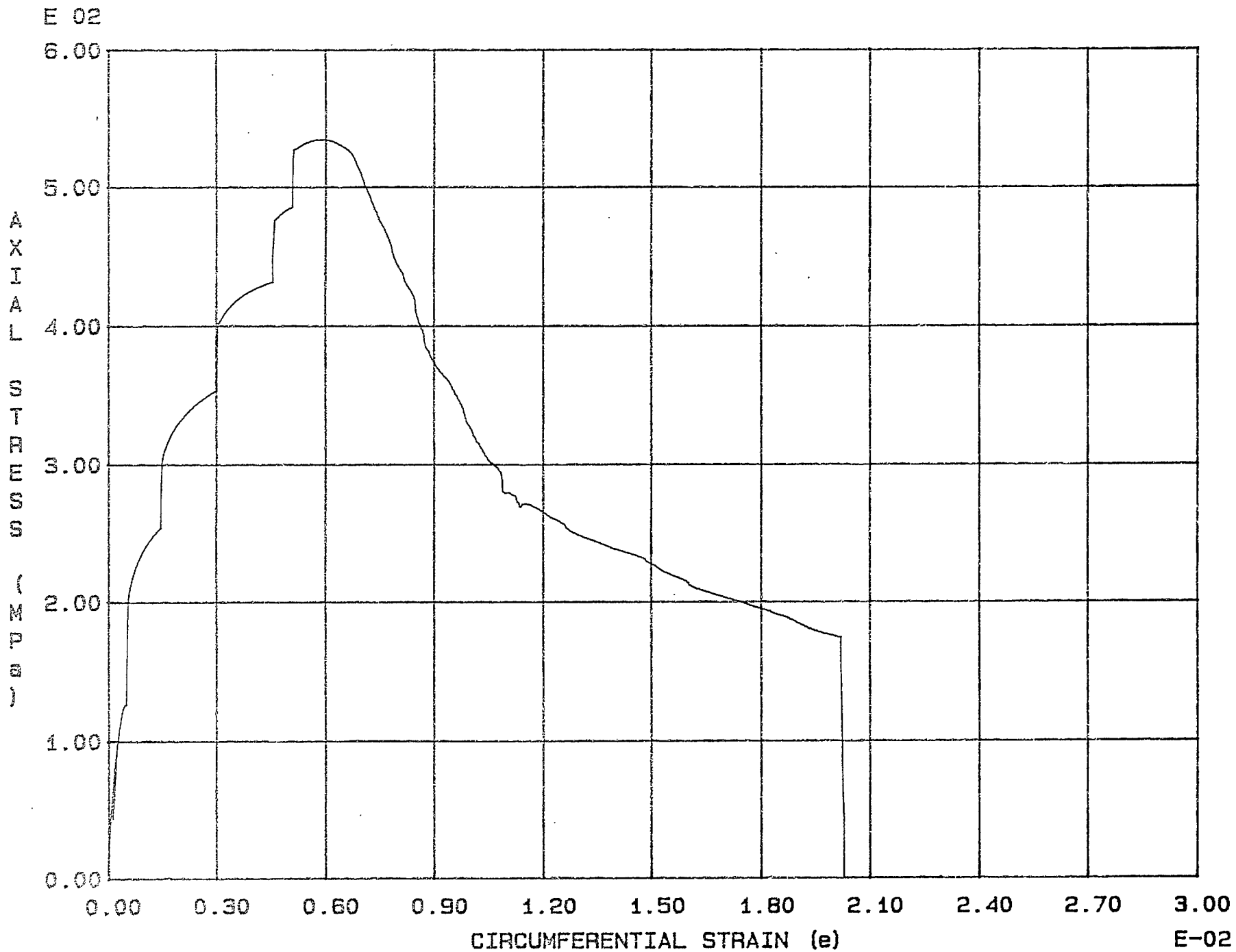

Fig. C - 5 Specimen G23

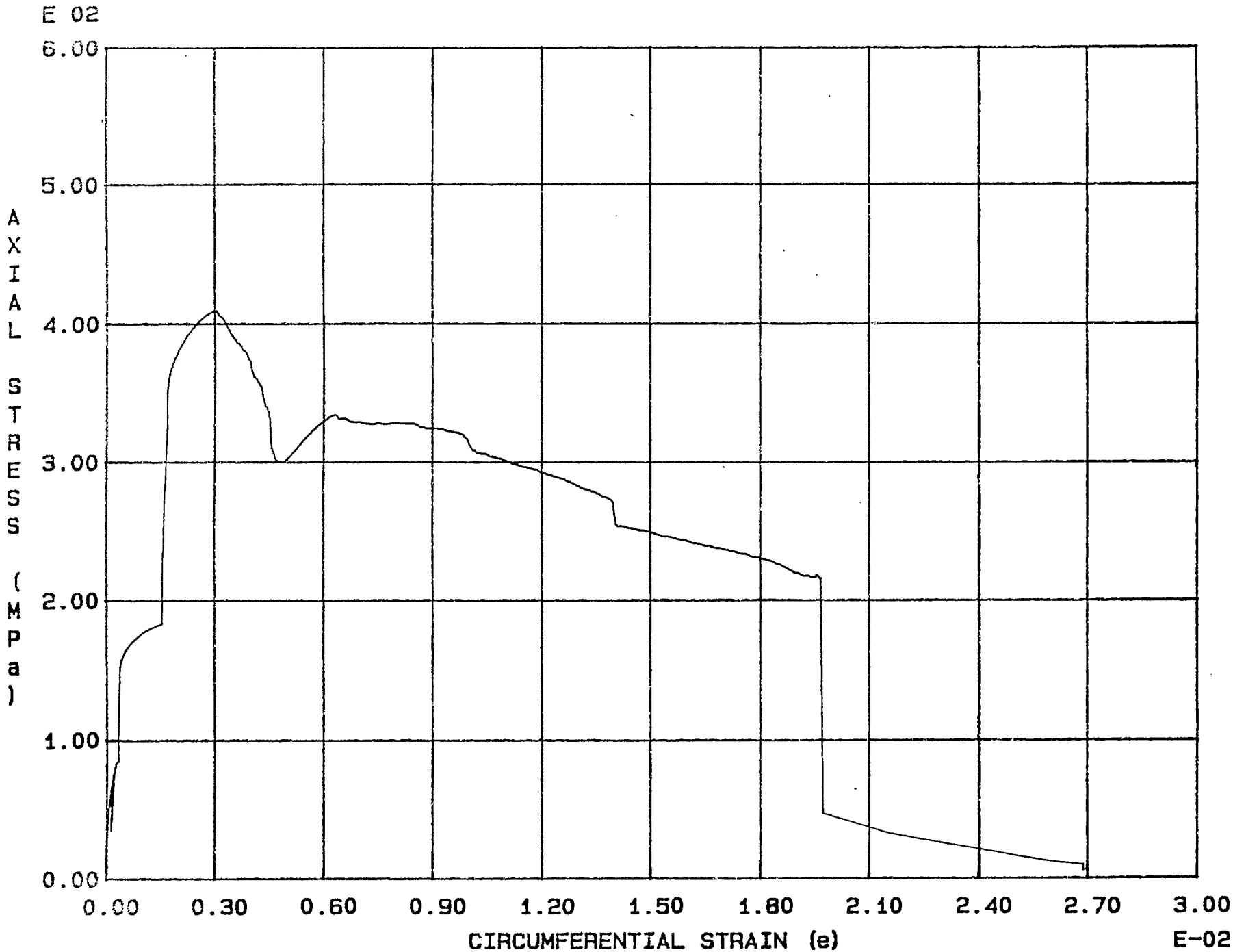

Fig. C - 6 Specimen G24

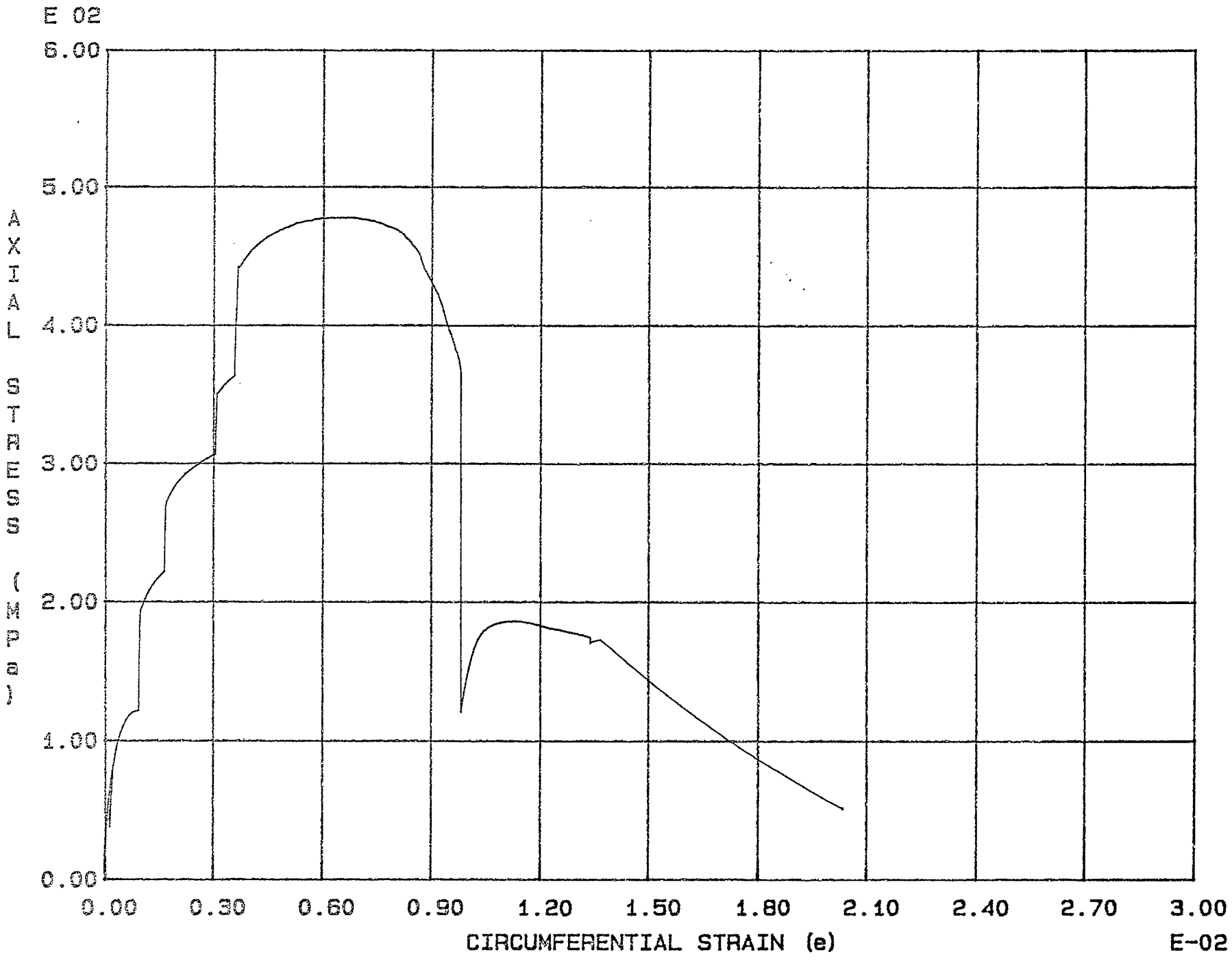

Fig. C - 7 Specimen G25

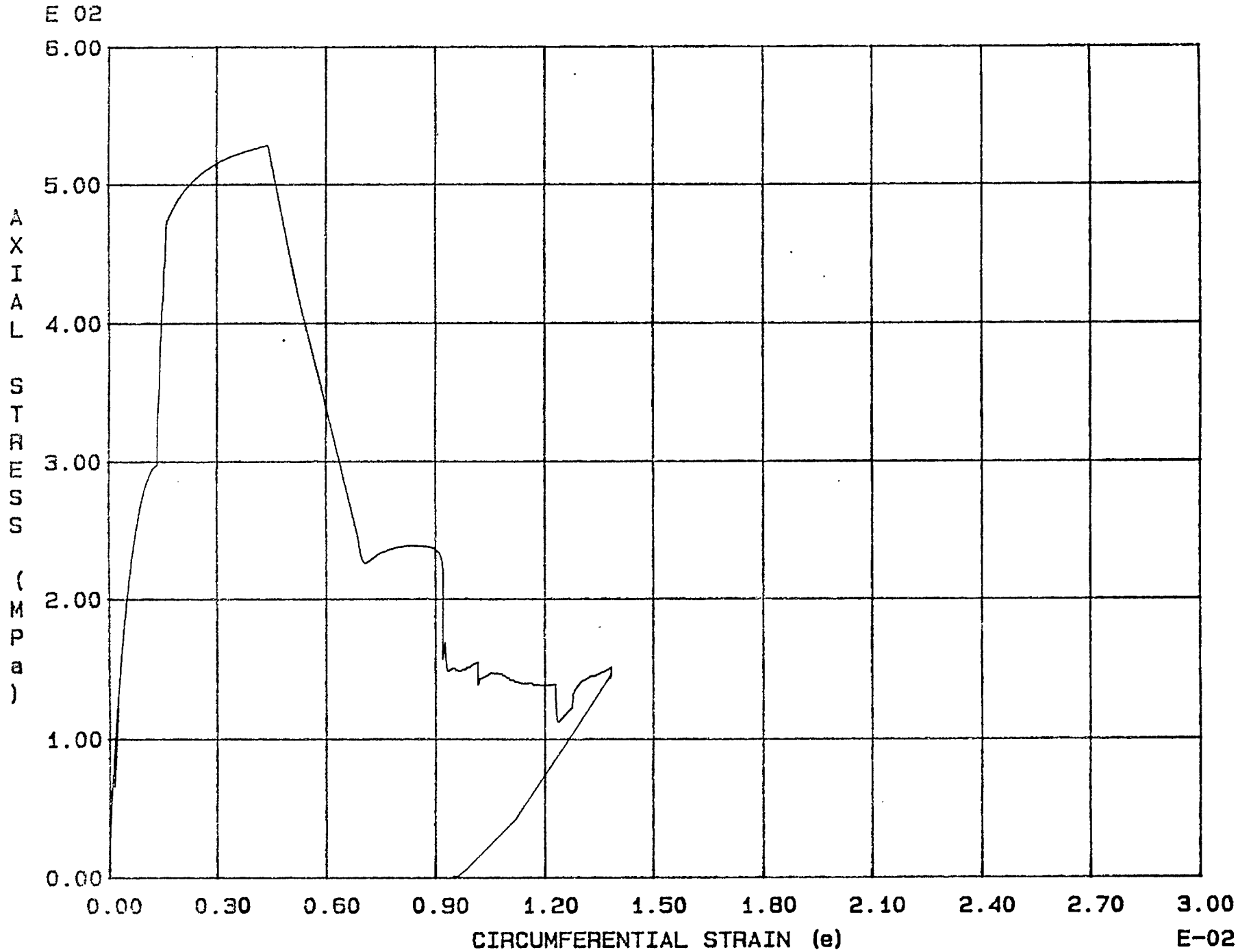

Fig. C - 8 Specimen D26

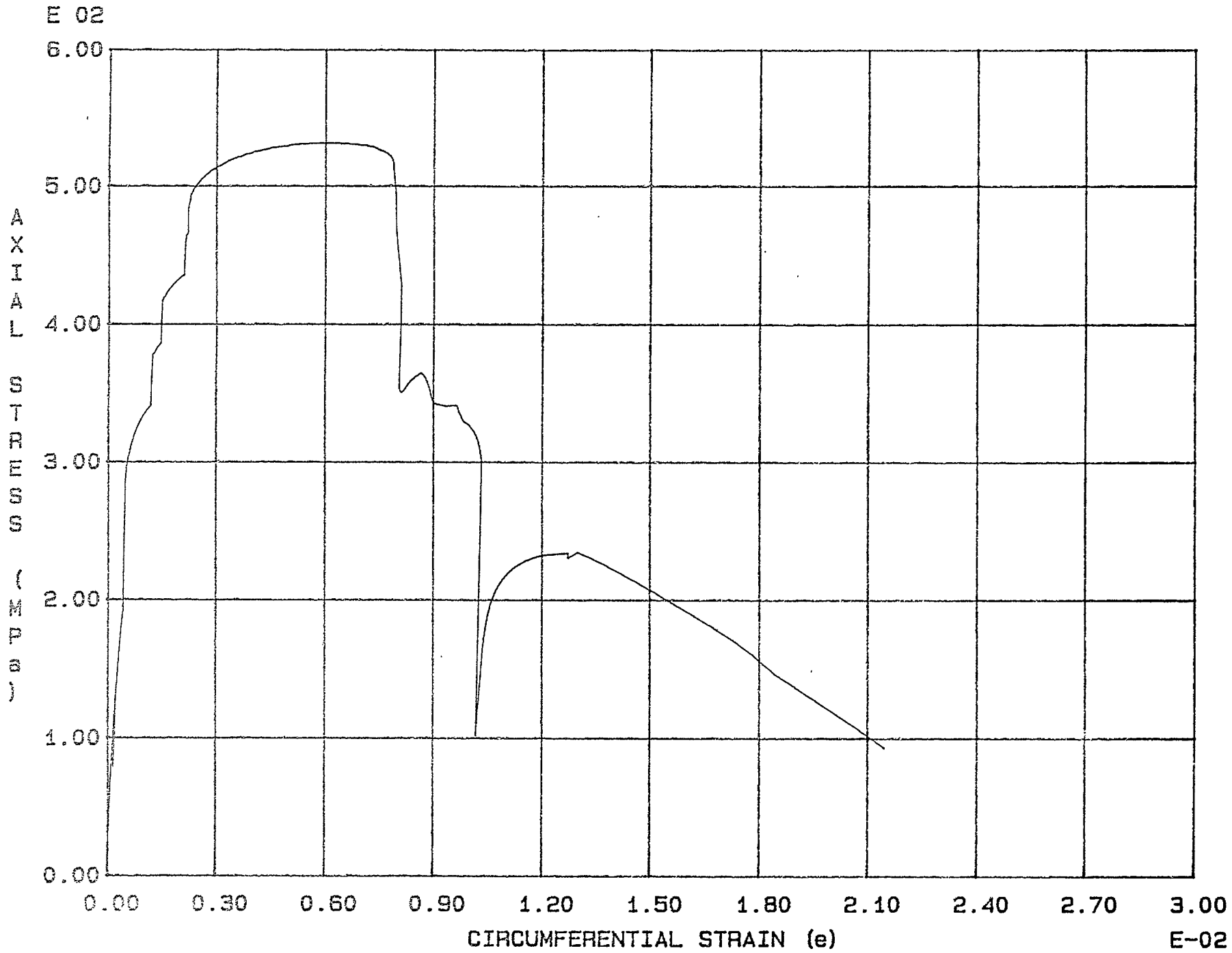

Fig. C - 9 Specimen D27

APPENDIX D

STRESS-CONFINING PRESSURE RESULTS

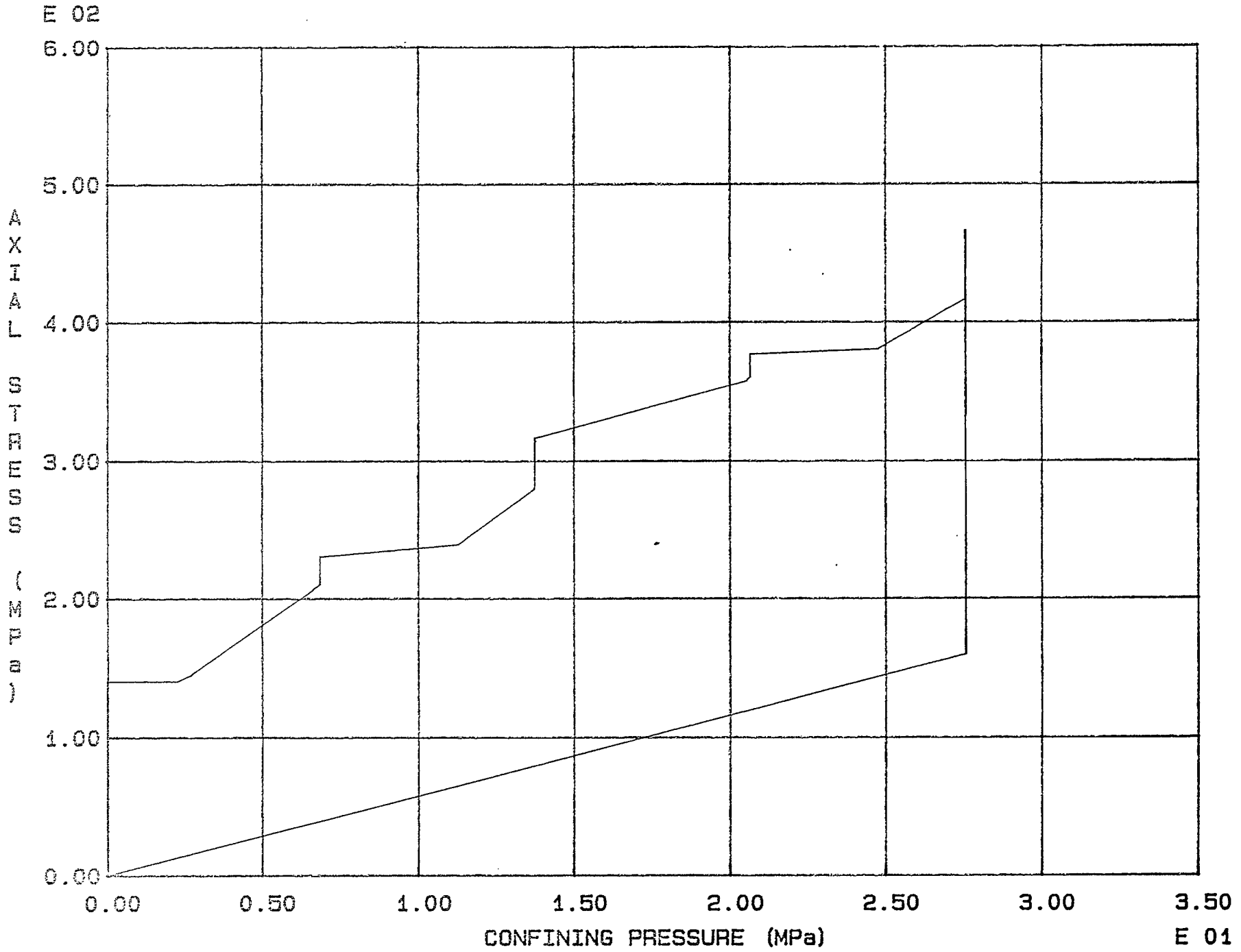

Fig. D - 1 Specimen G19

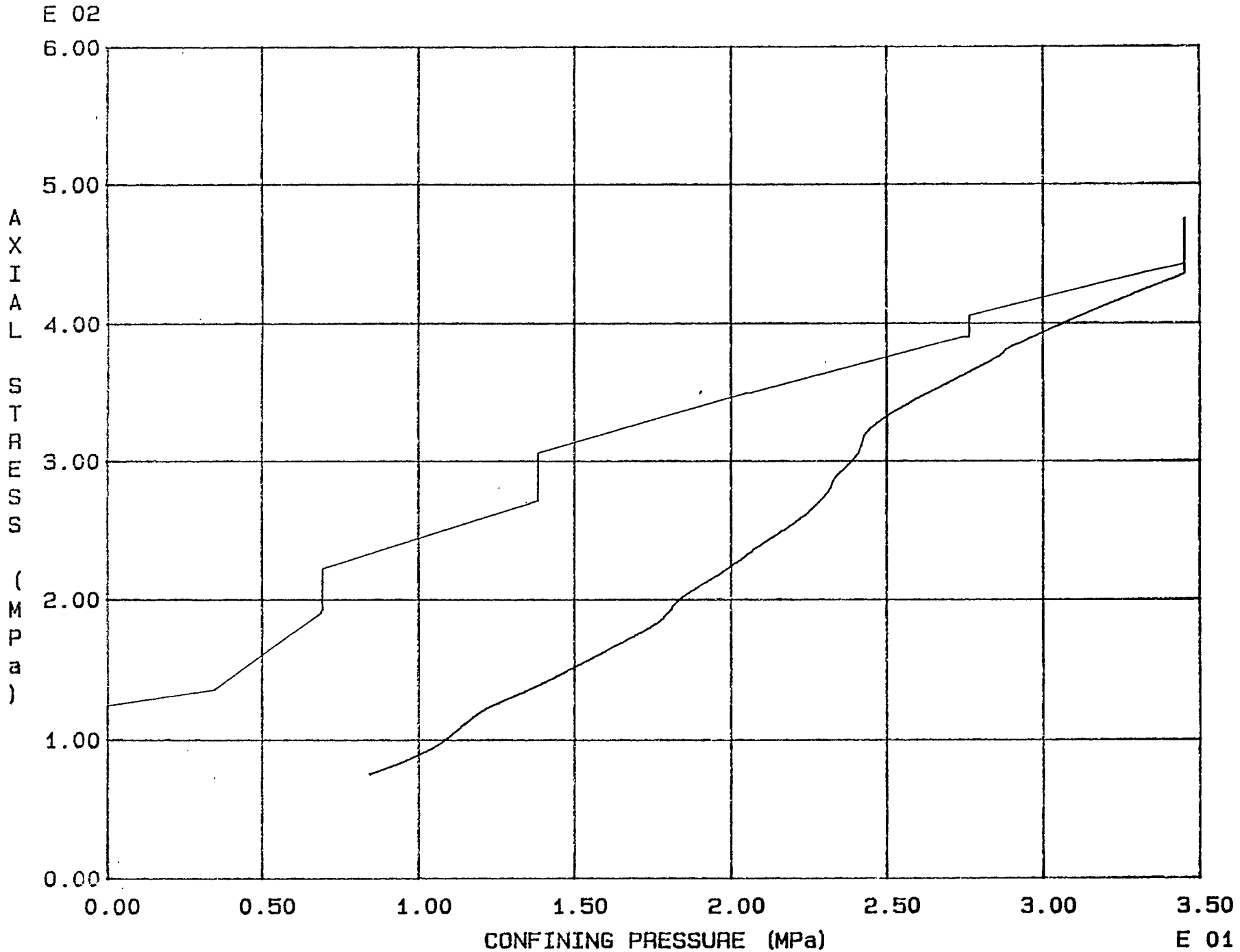

Fig. D - 2 Specimen G20

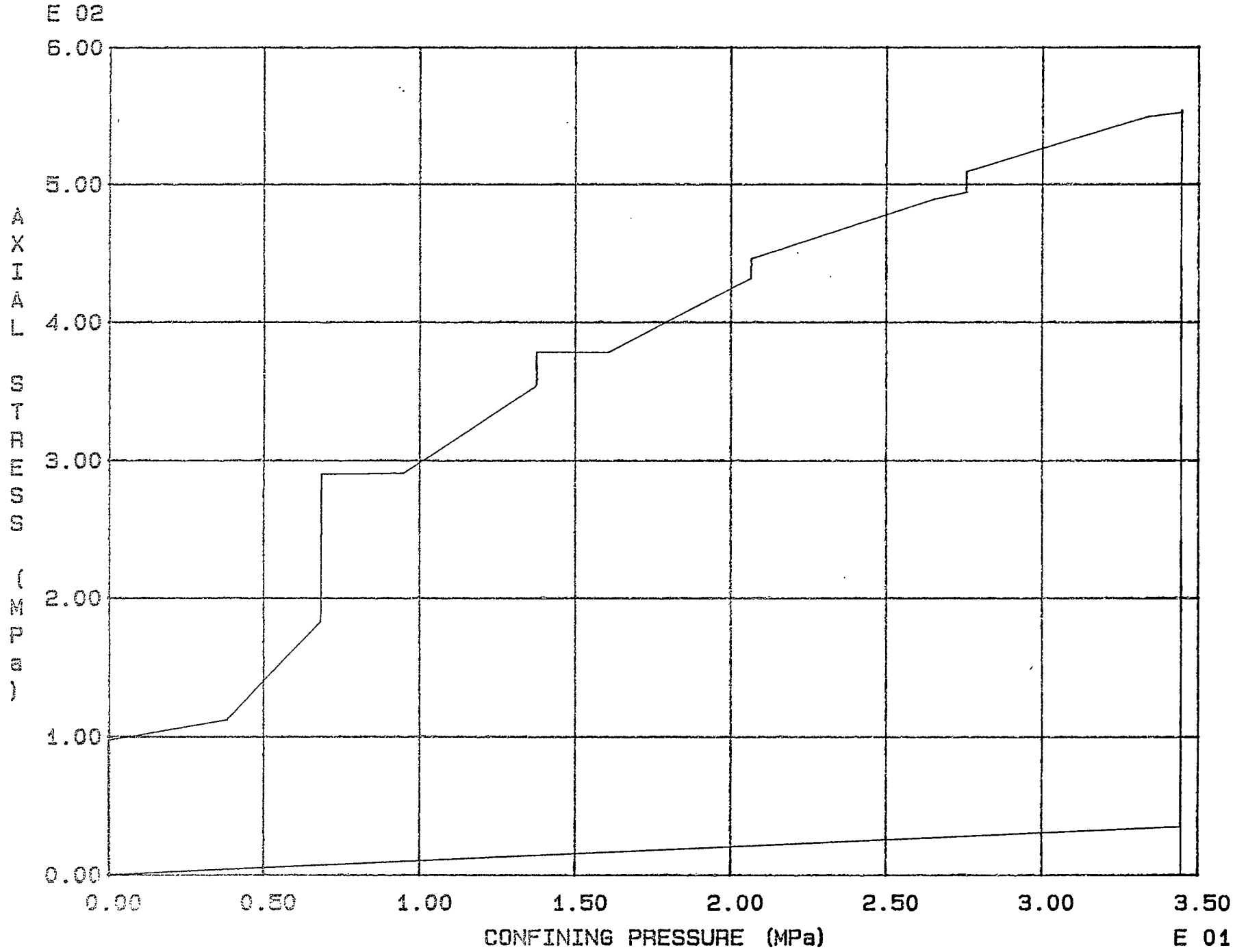

Fig. D - 3 Specimen G21

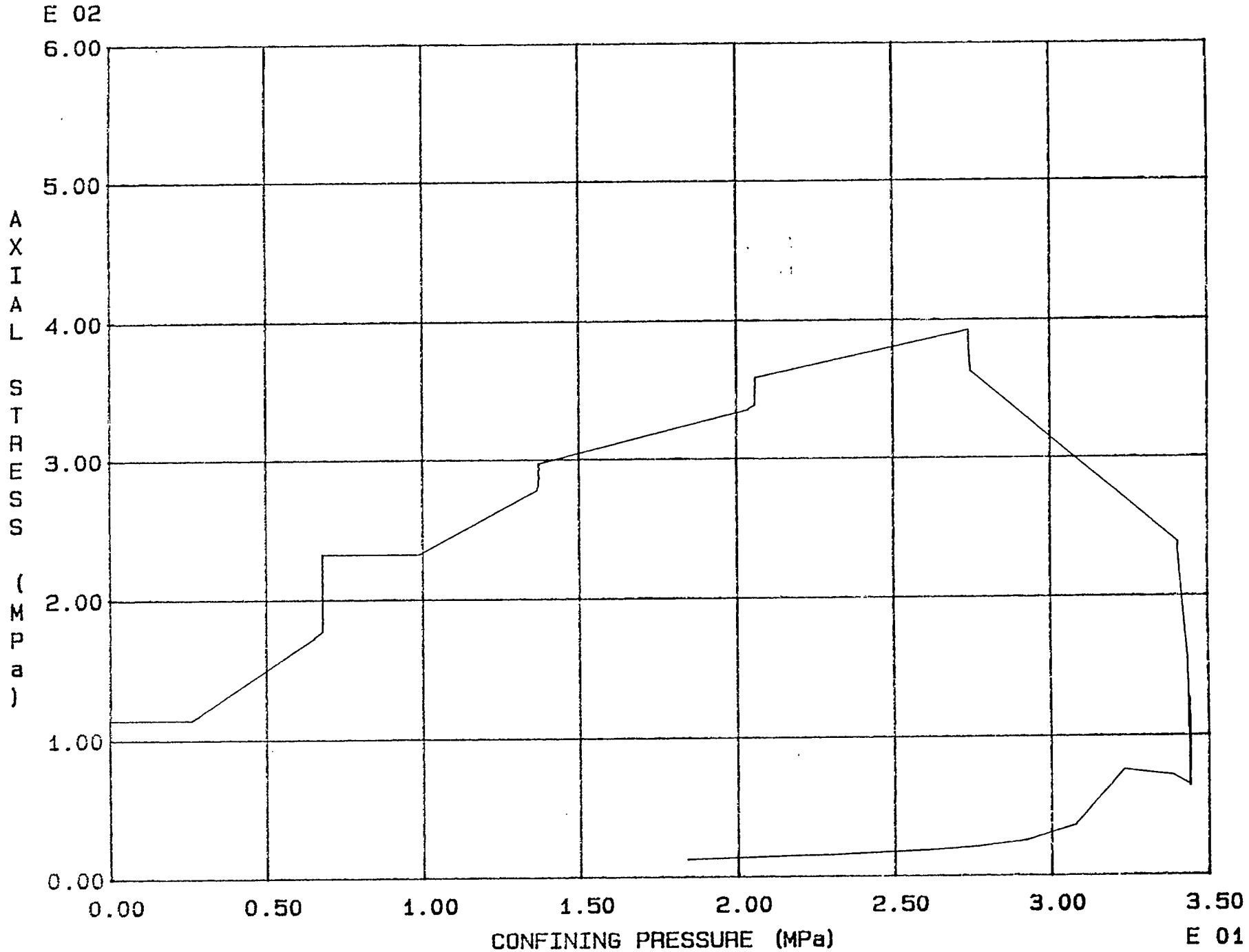

Fig. D - 4 Specimen G22

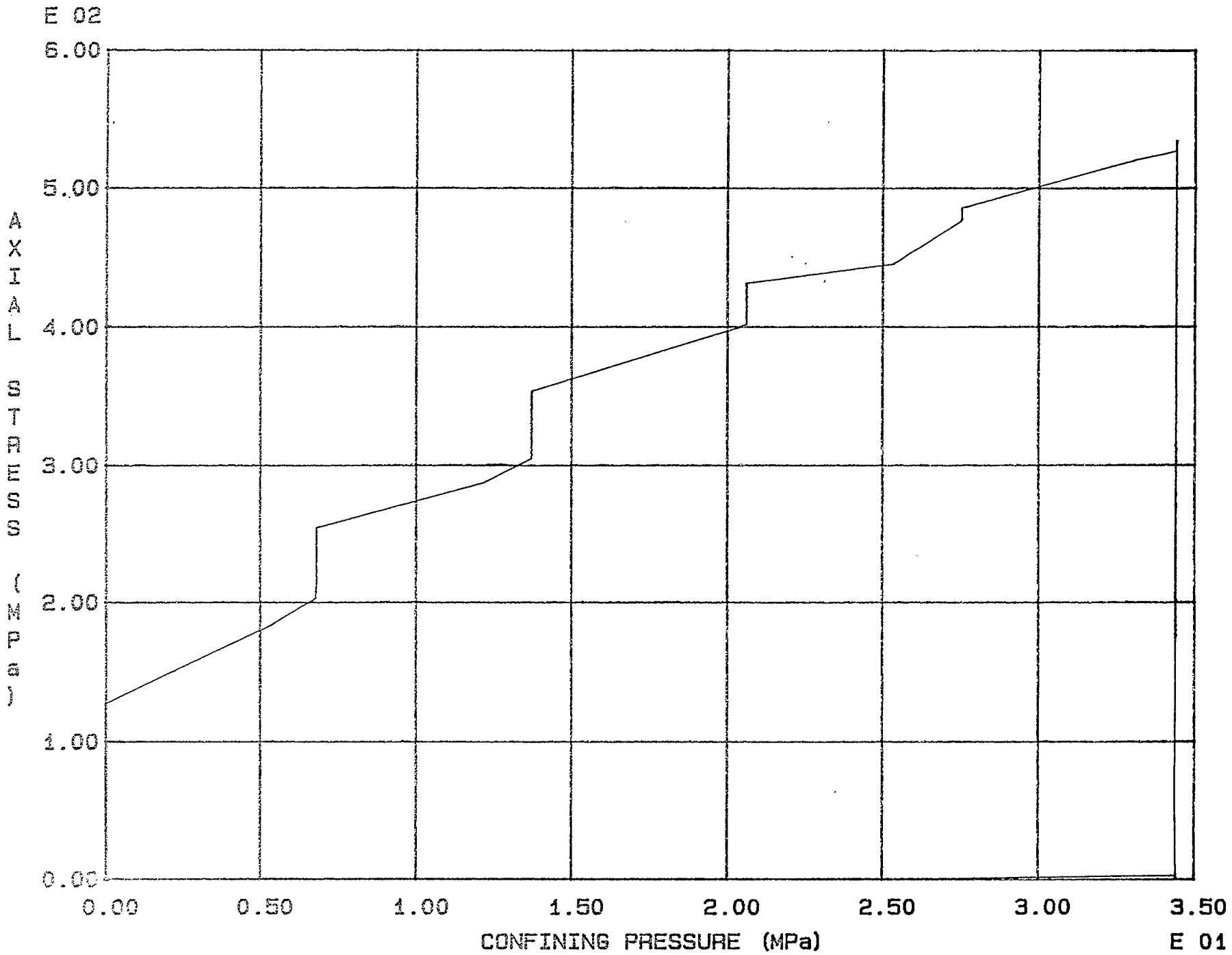

Fig. D - 5 Specimen G23

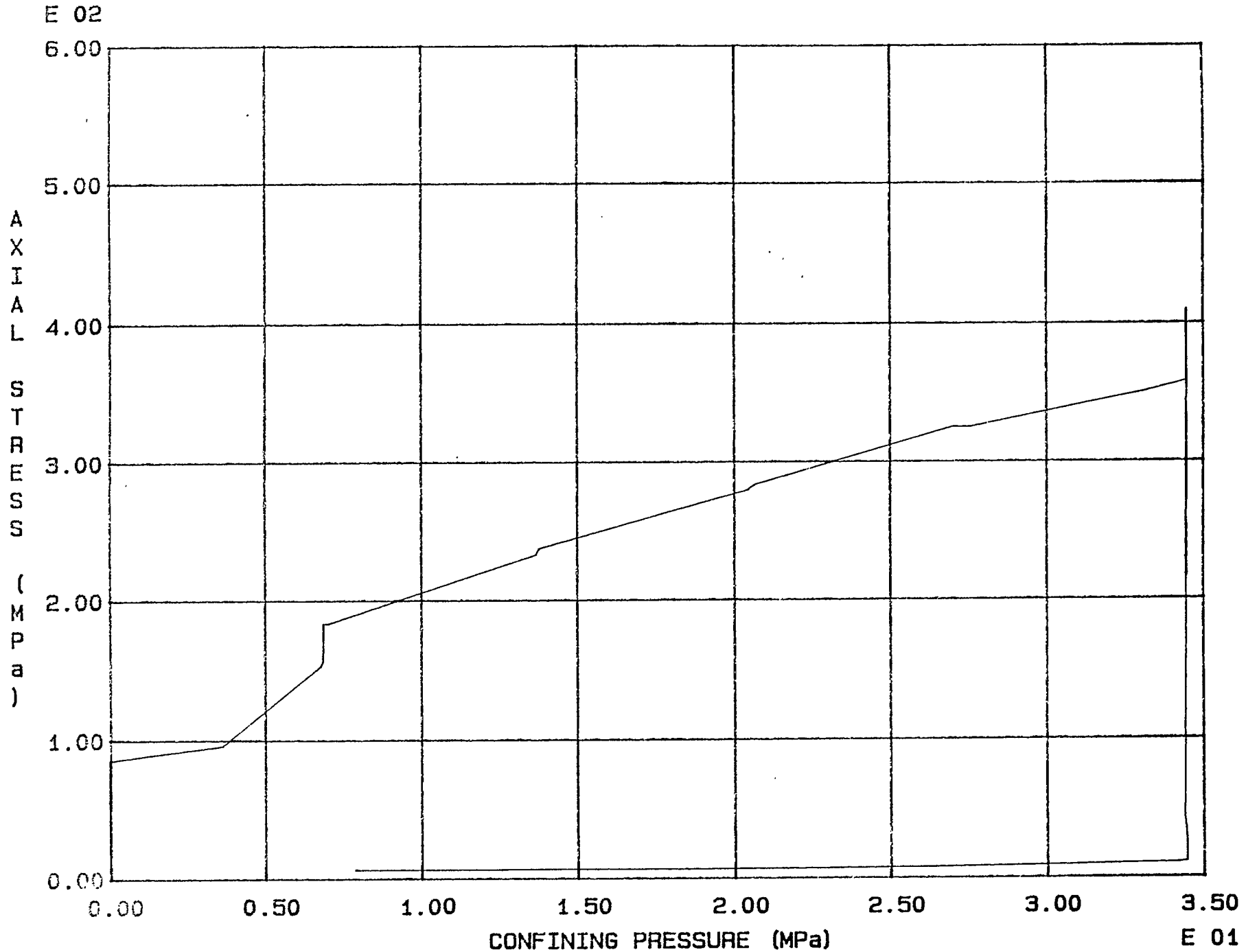

Fig. D - 6 Specimen G24

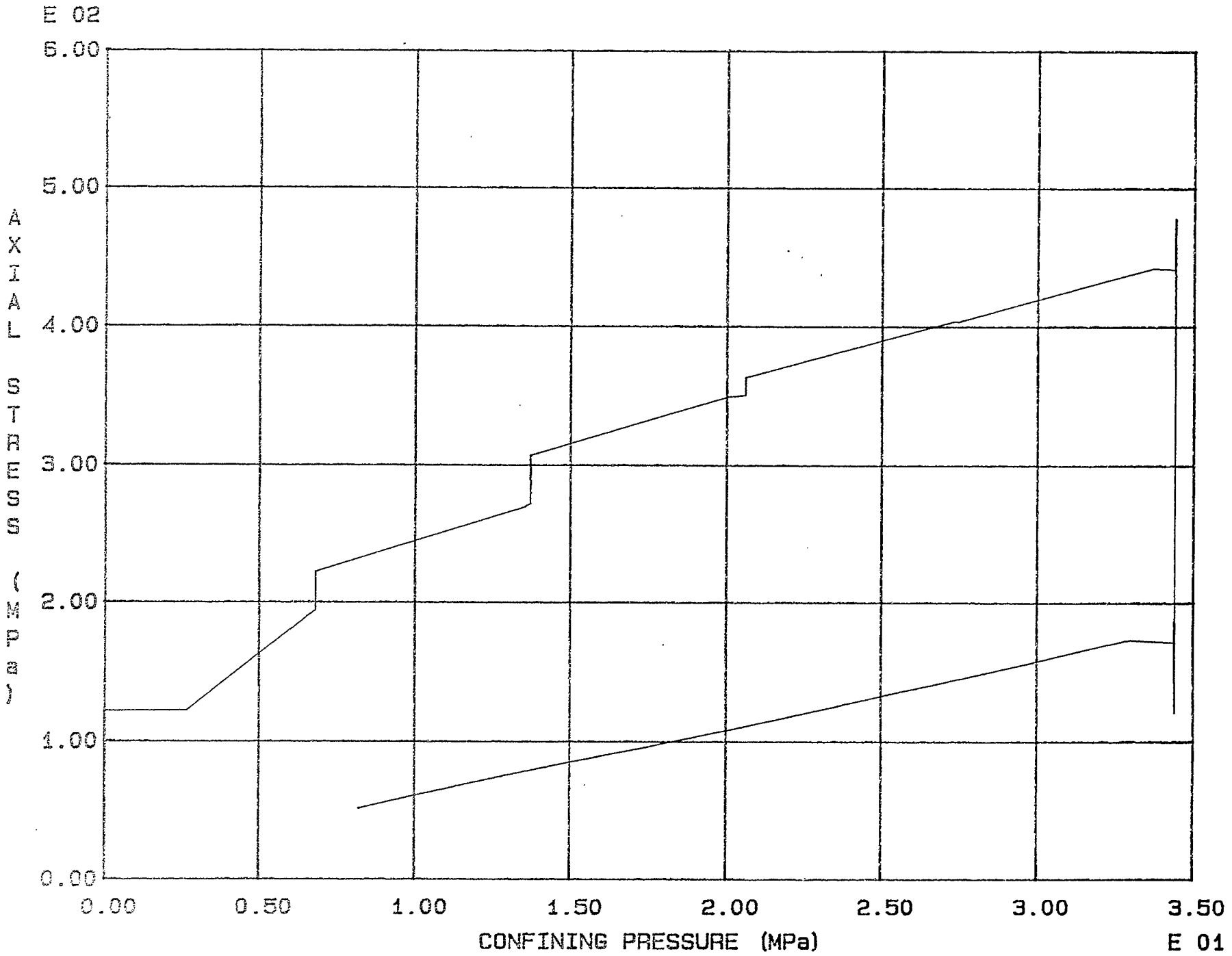

Fig. D - 7 Specimen G25

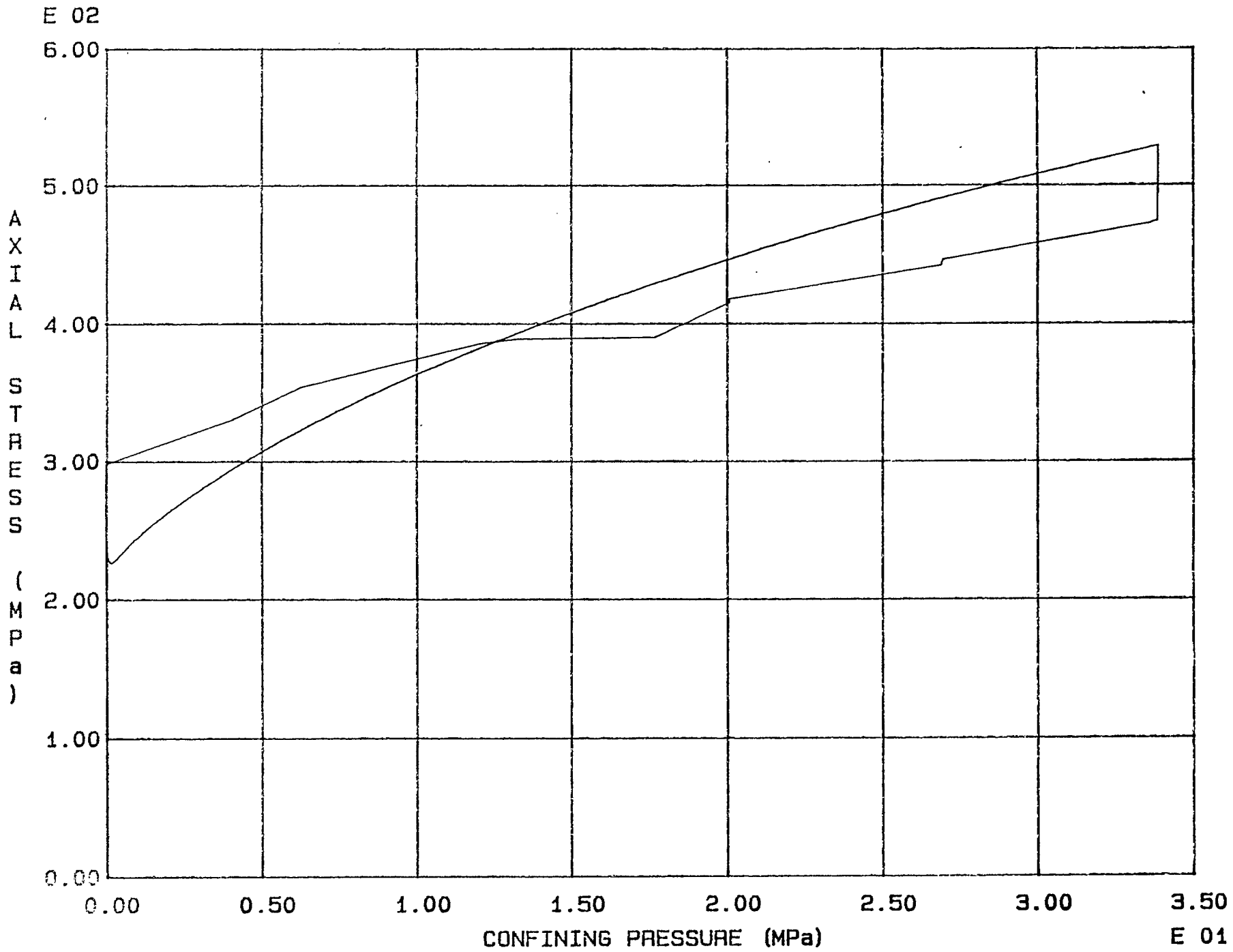

Fig. D - 8 Specimen D26

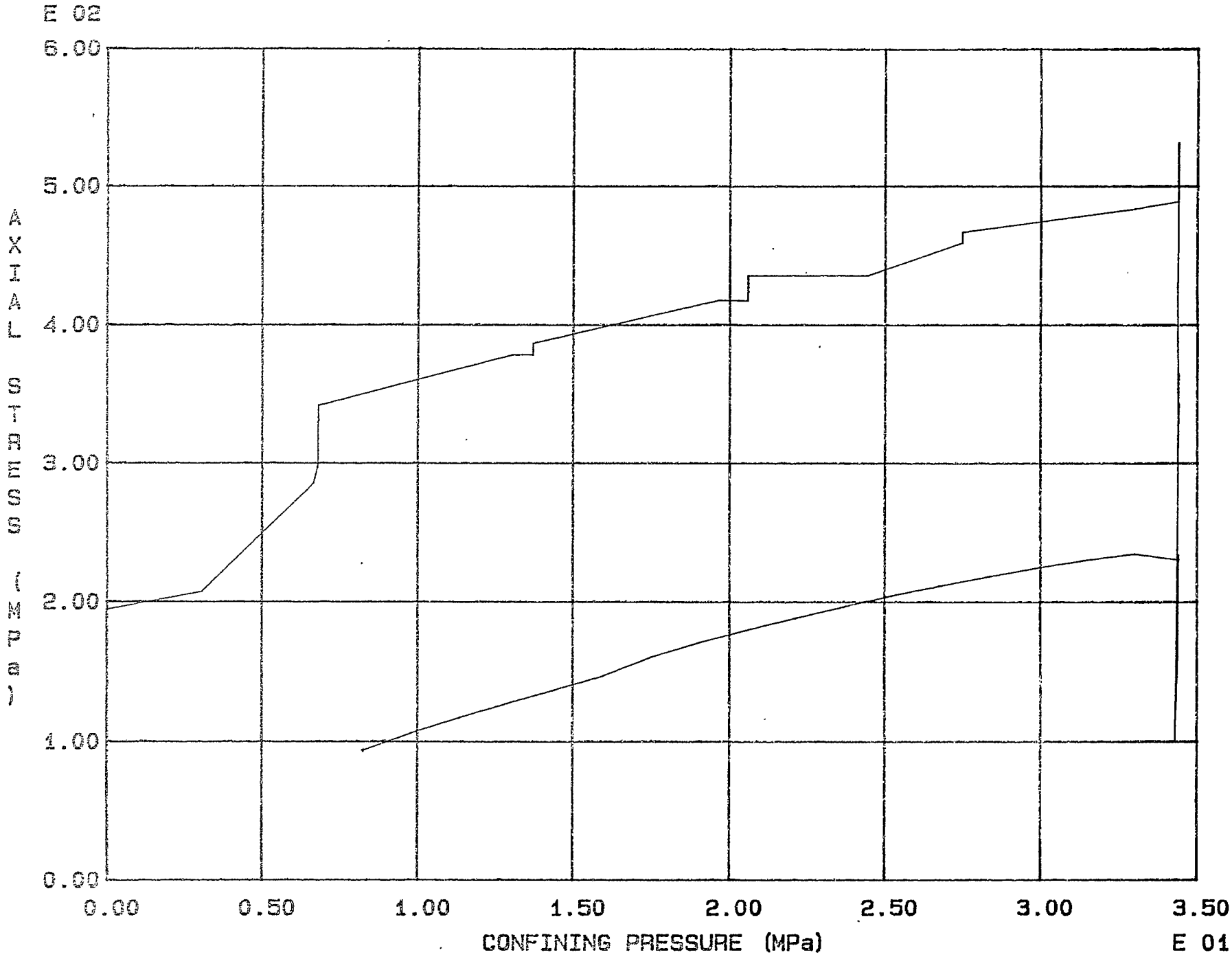

Fig. D - 9 Specimen D27

MOHR ENVELOPE

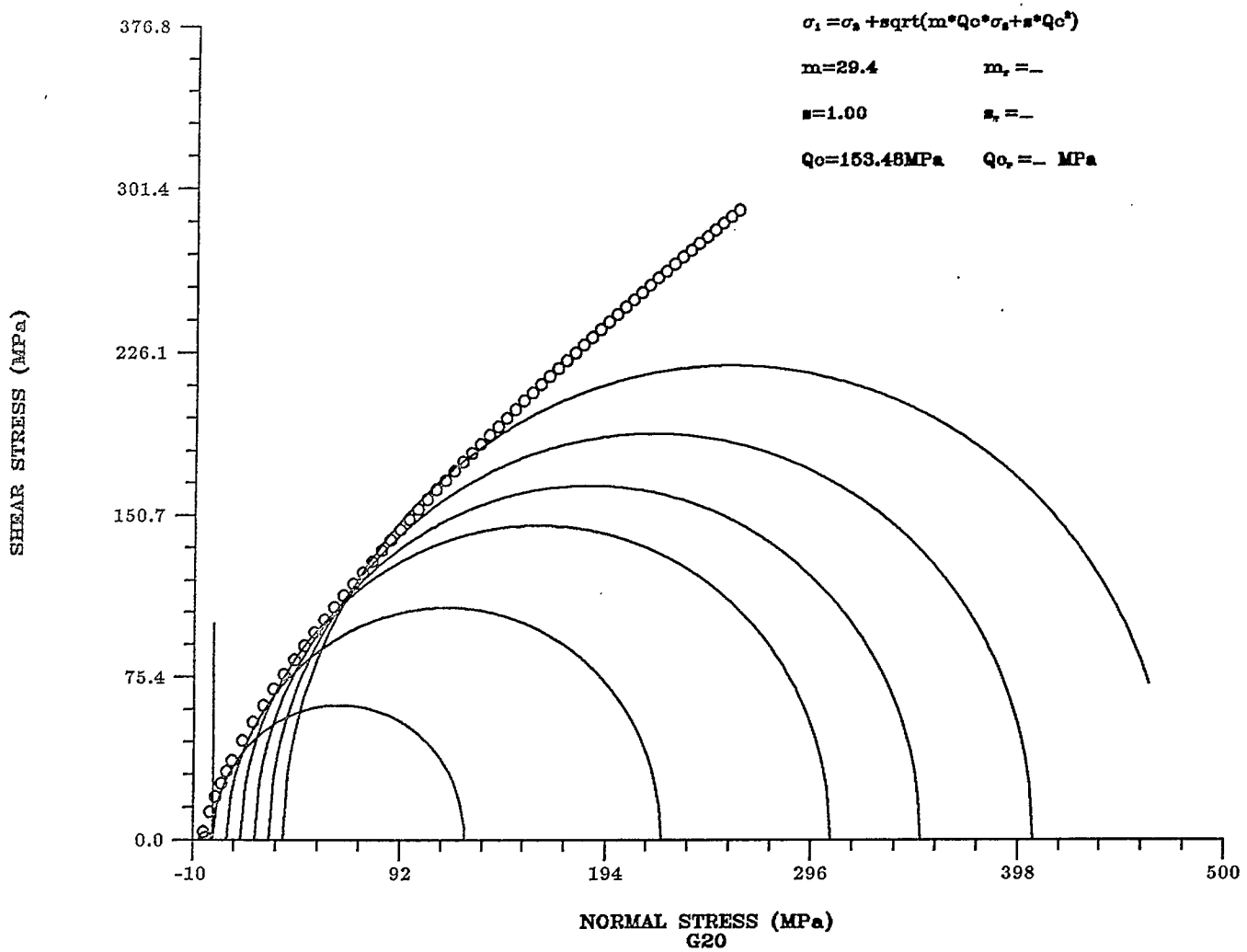

Fig. A - 2 Specimen G20

MOHR ENVELOPE

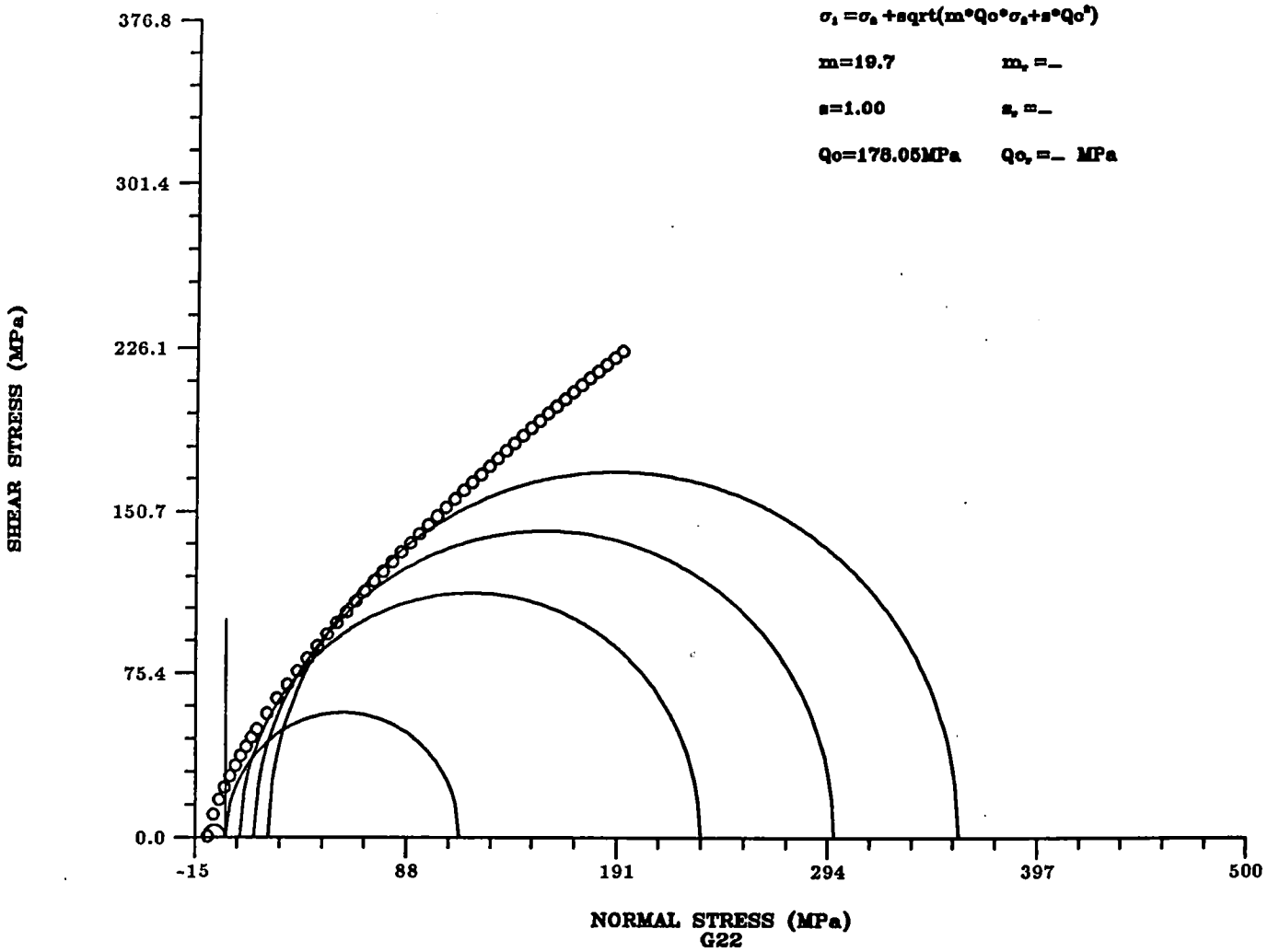

Fig. A - 4 Specimen G22

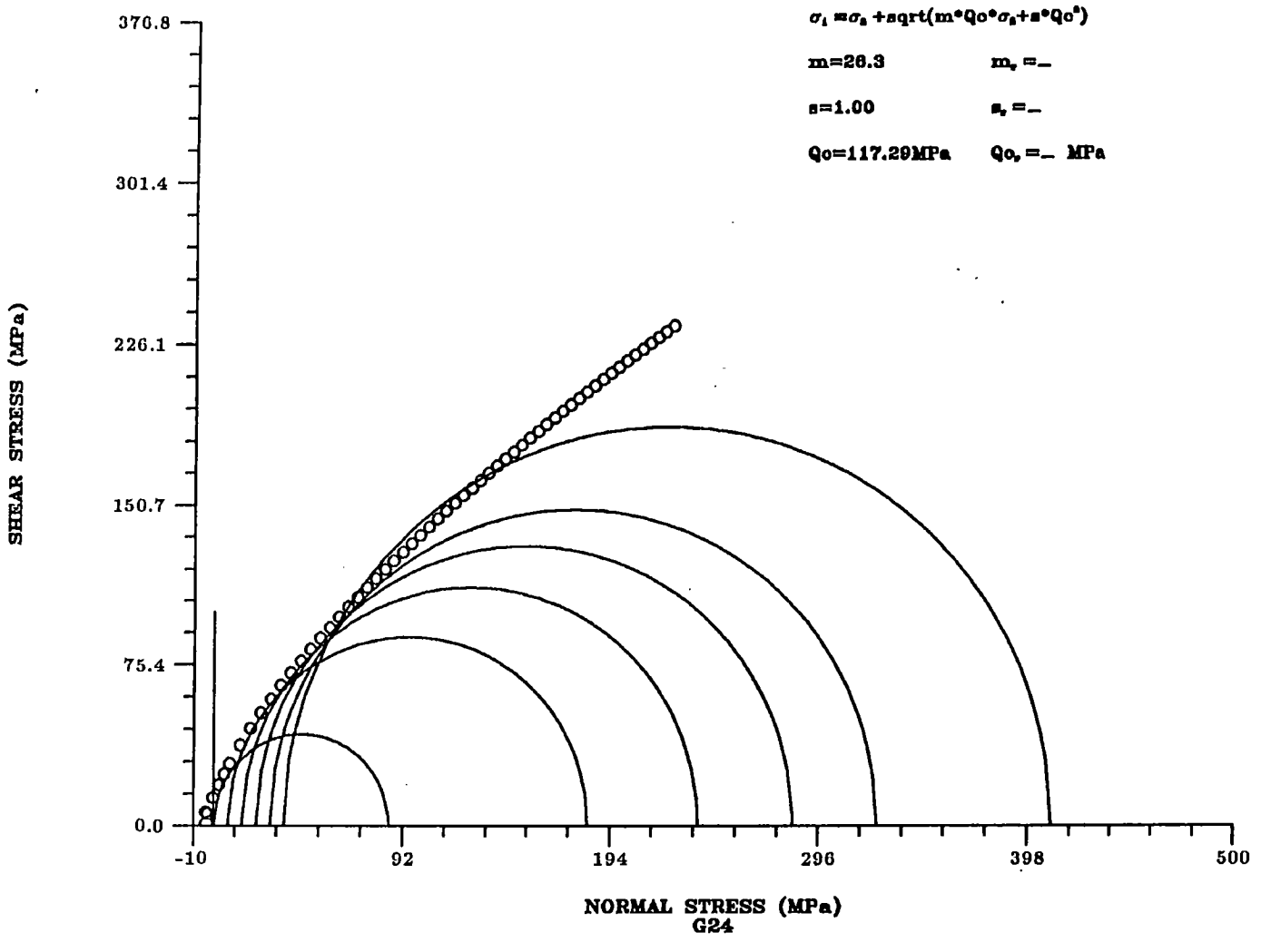

Fig. A - 6 Specimen G24

MOHR ENVELOPE

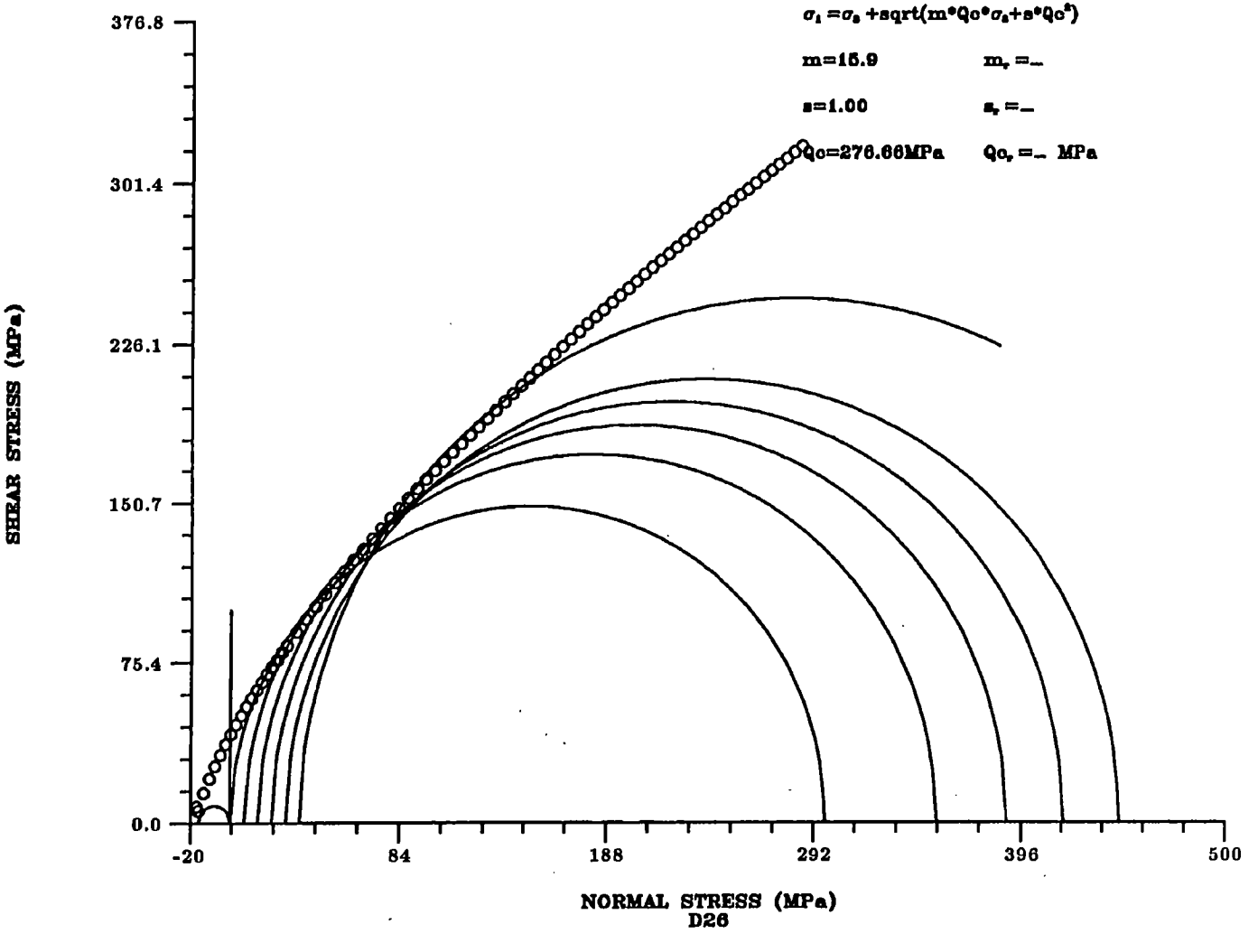

Fig. A - 8 Specimen D26

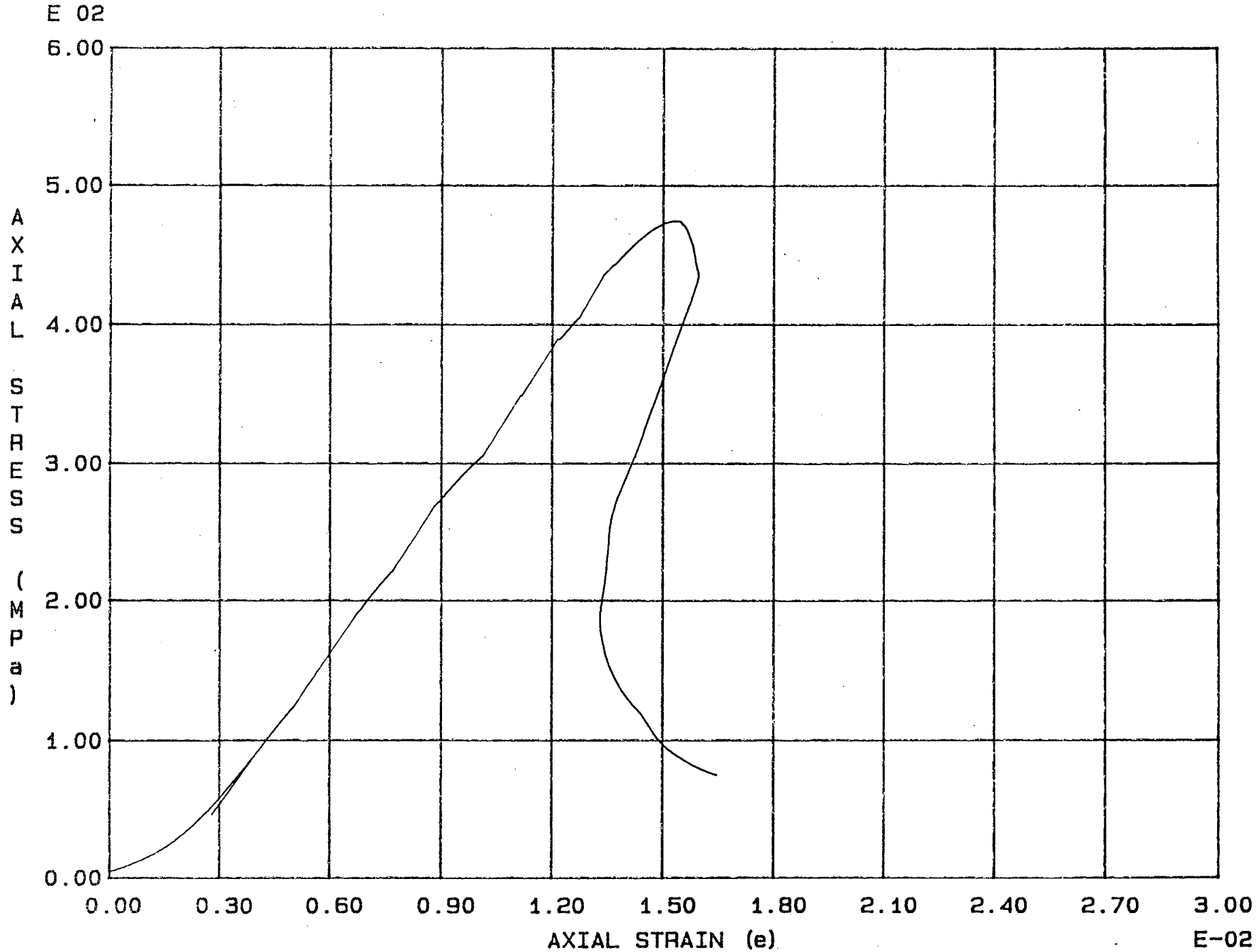

Fig. B - 2 Specimen G20

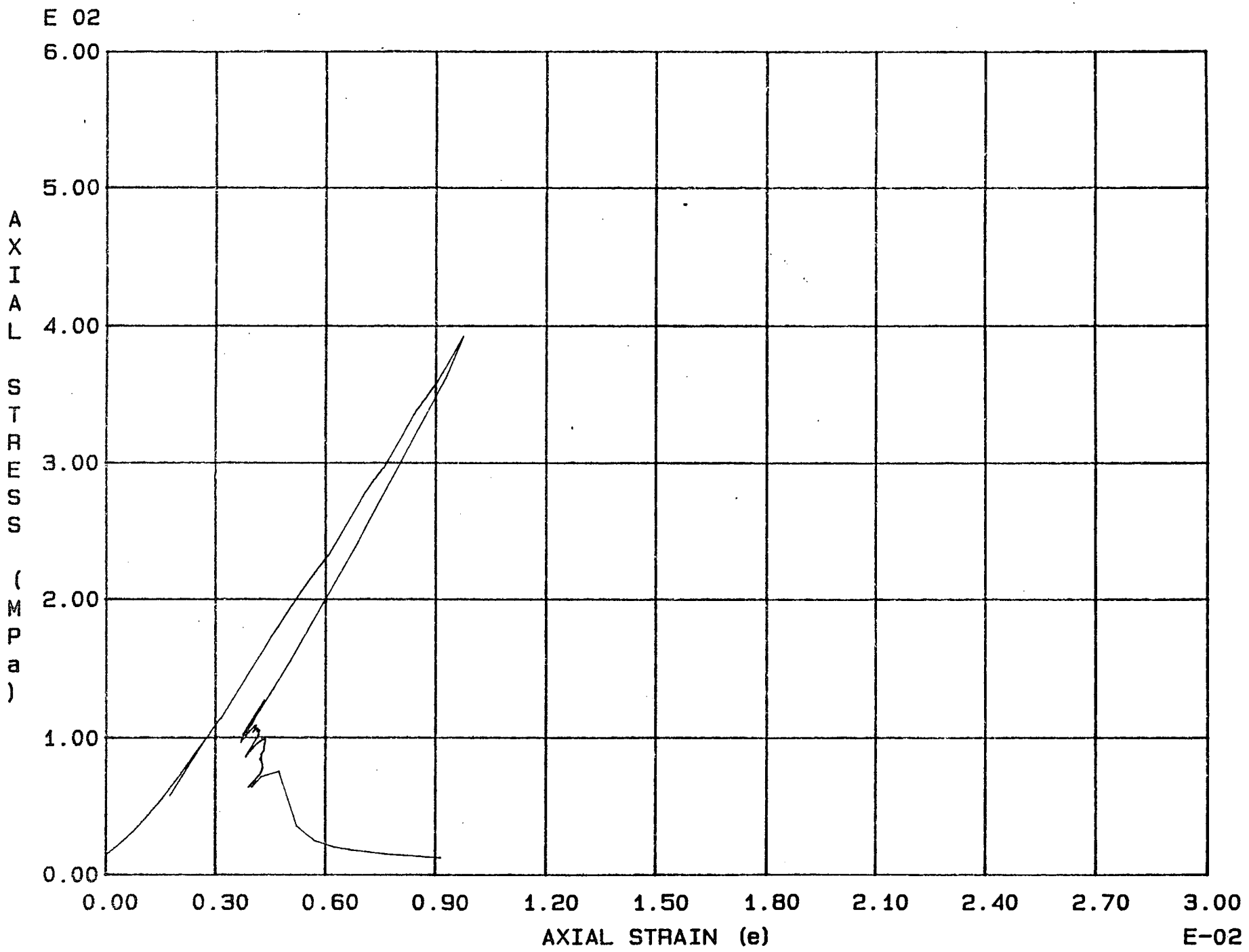

Fig. B - 4 Specimen G22

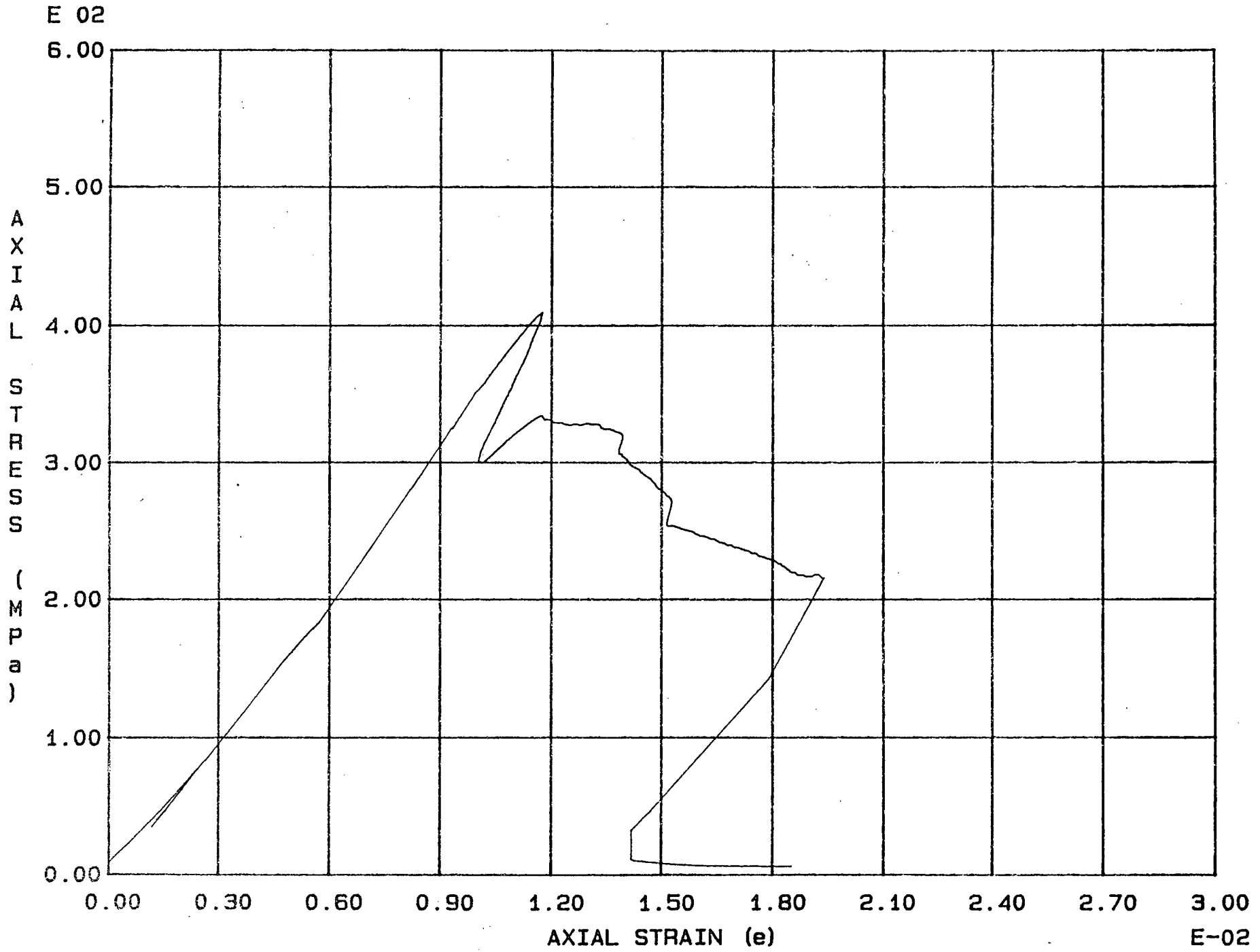

Fig. B - 6 Specimen G24

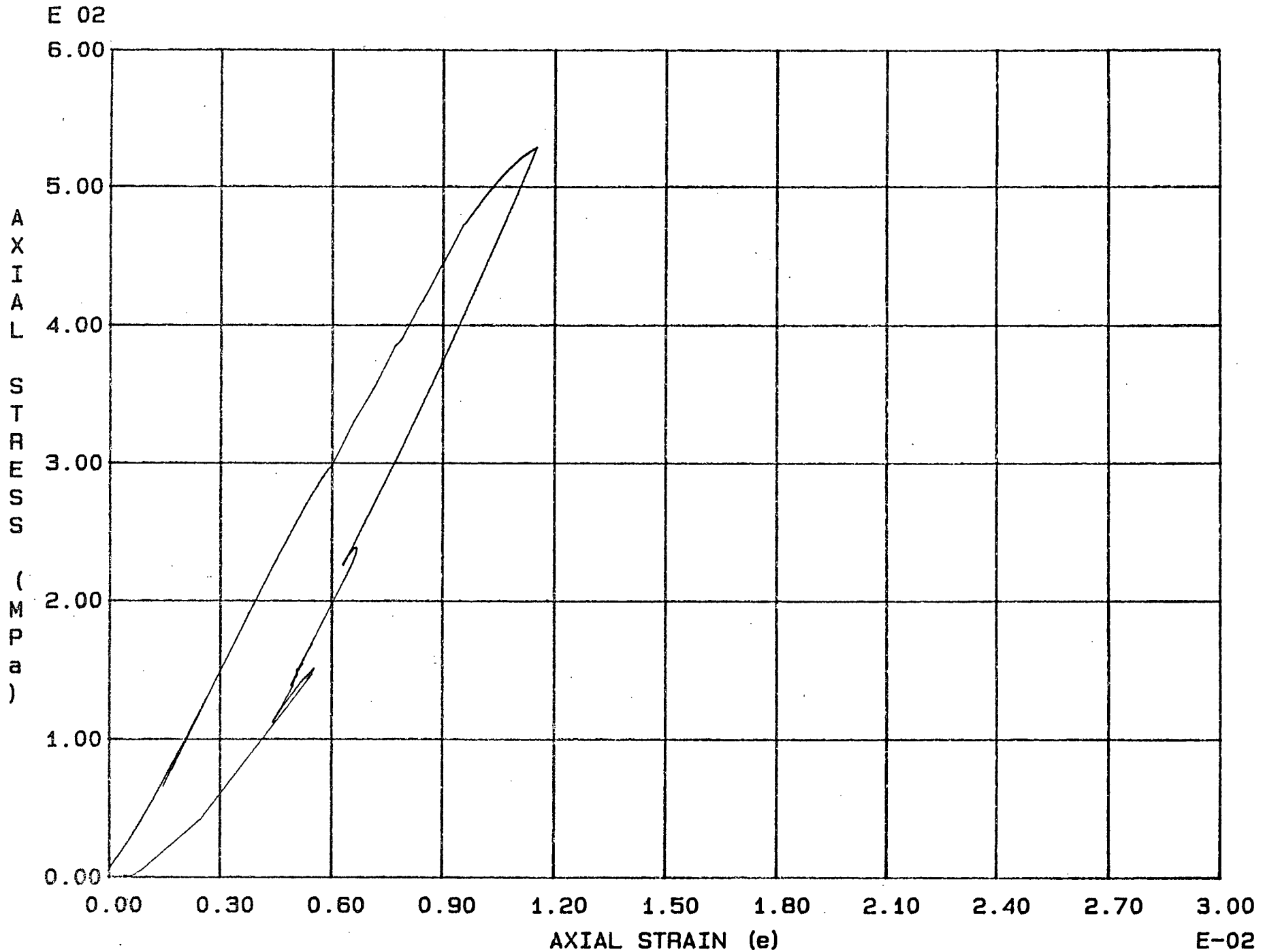

Fig. B - 8 Specimen D26

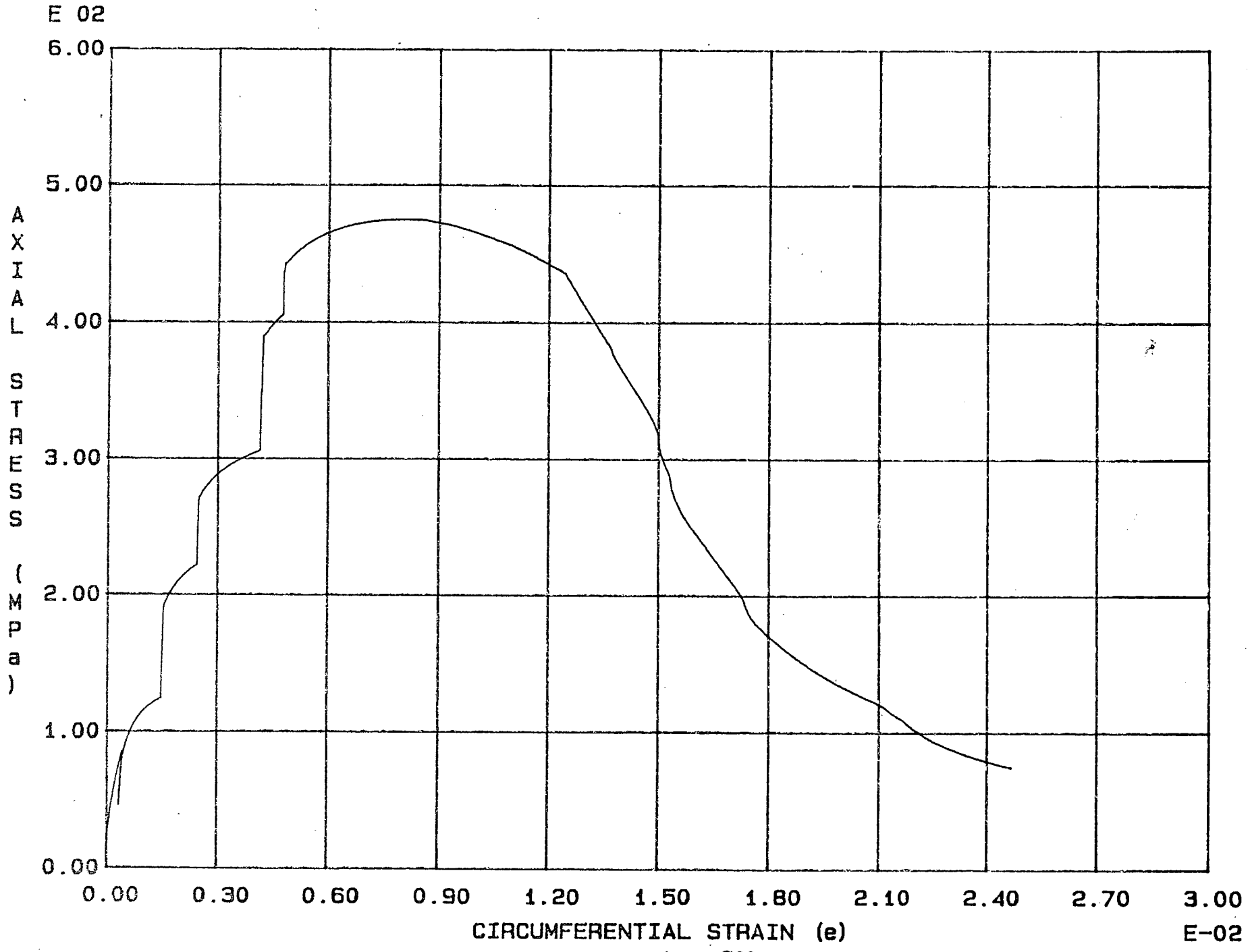

Fig. C - 2 Specimen G20

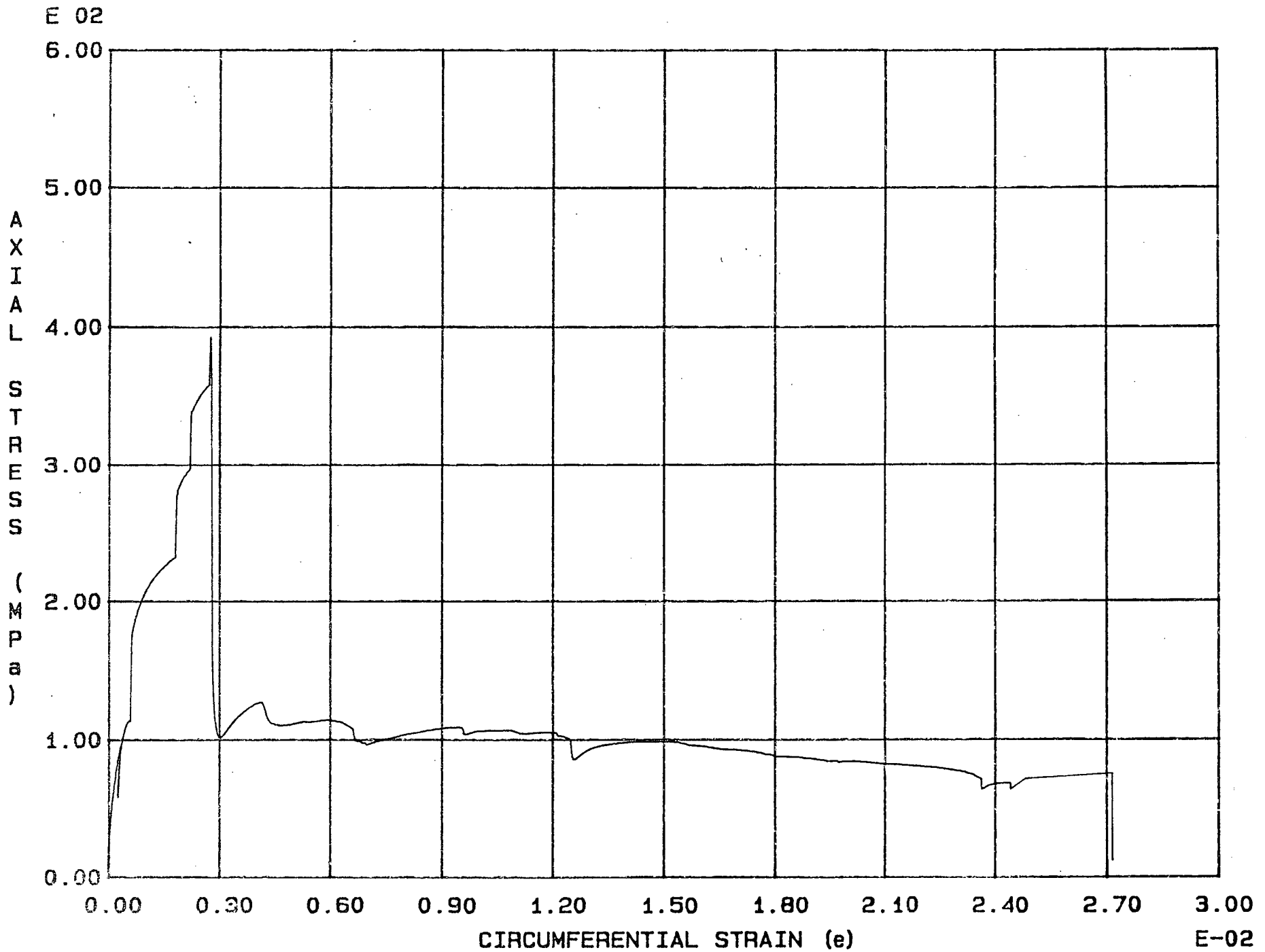

Fig. C - 4 Specimen G22

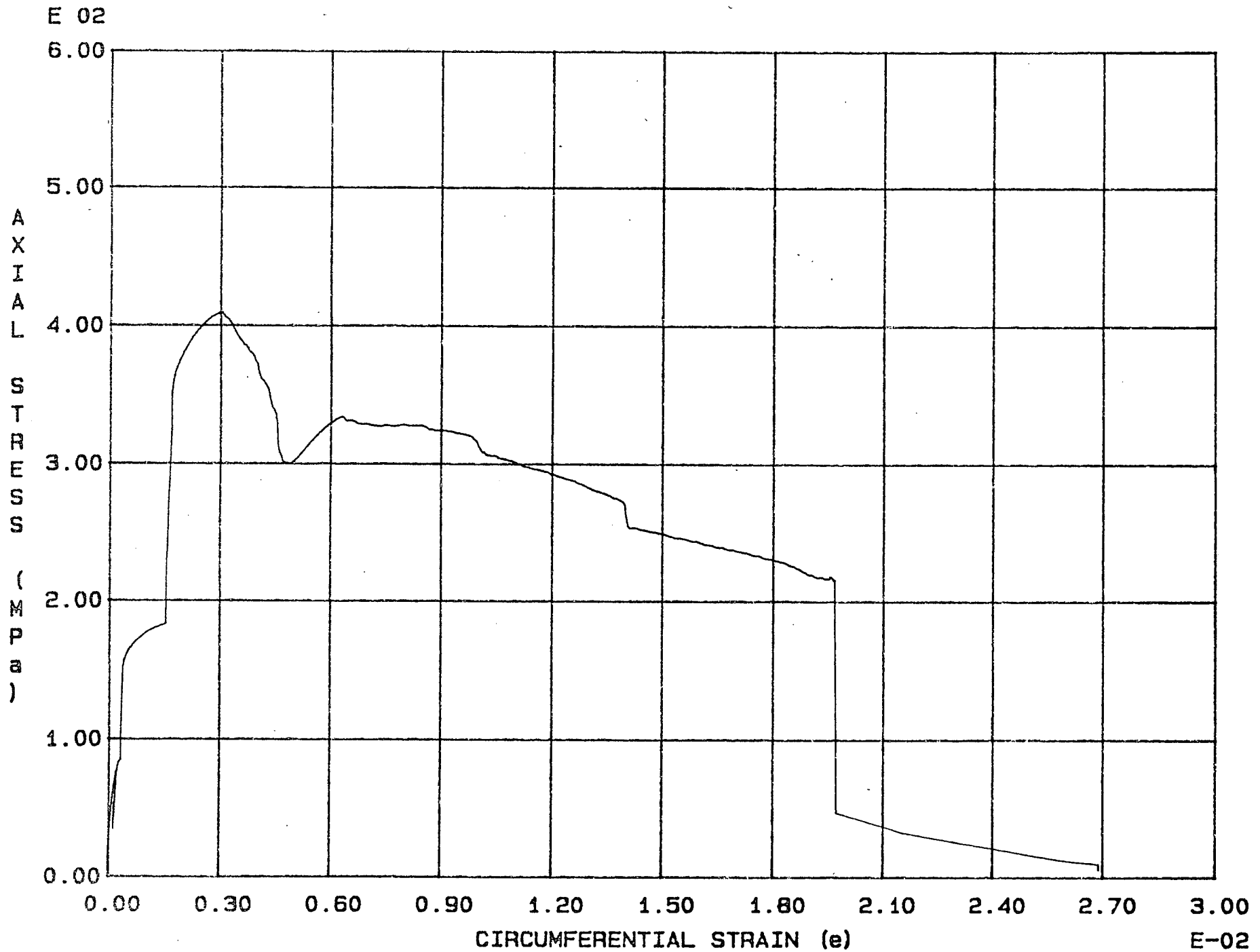

Fig. C - 6 Specimen G24

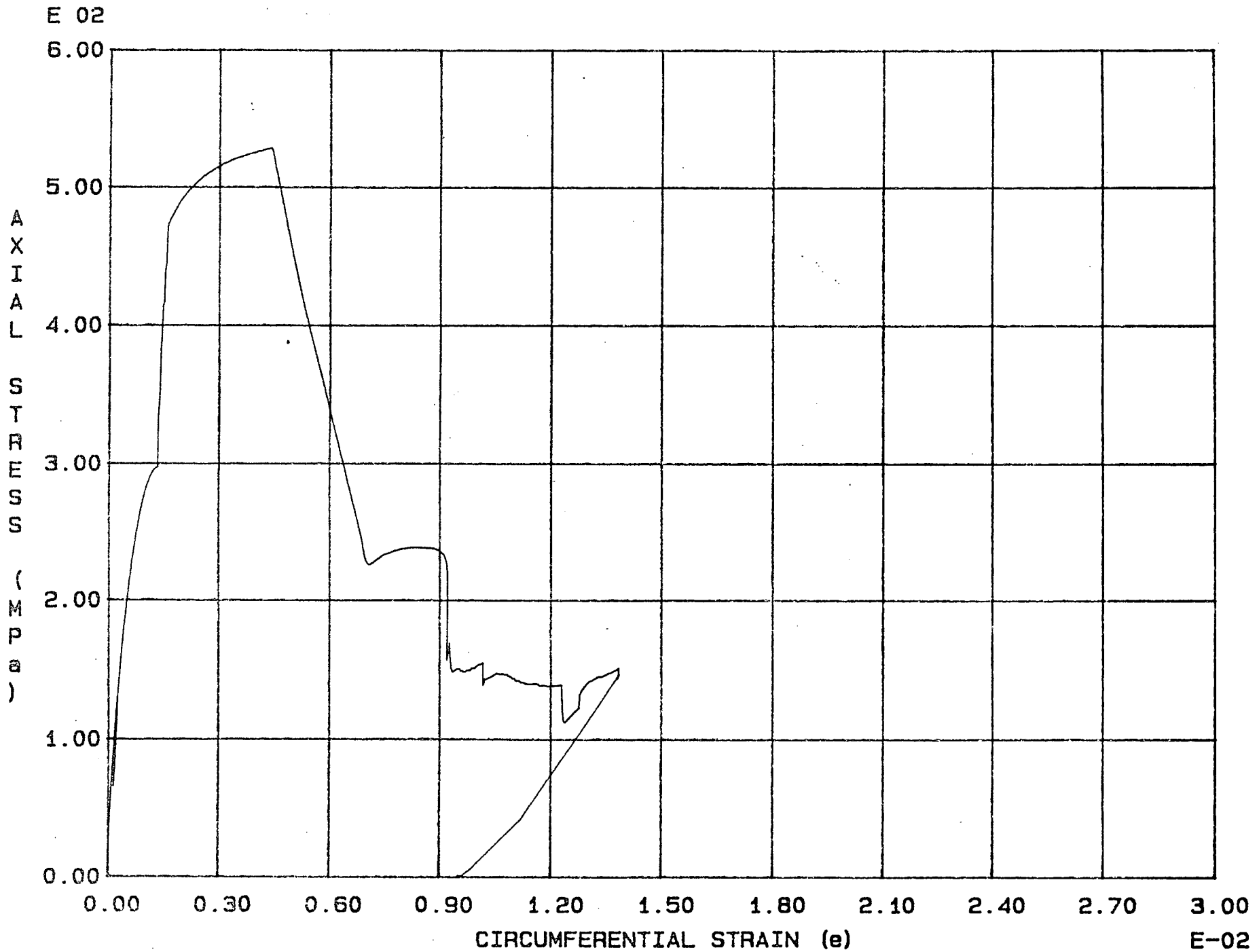

Fig. C - 8 Specimen D26

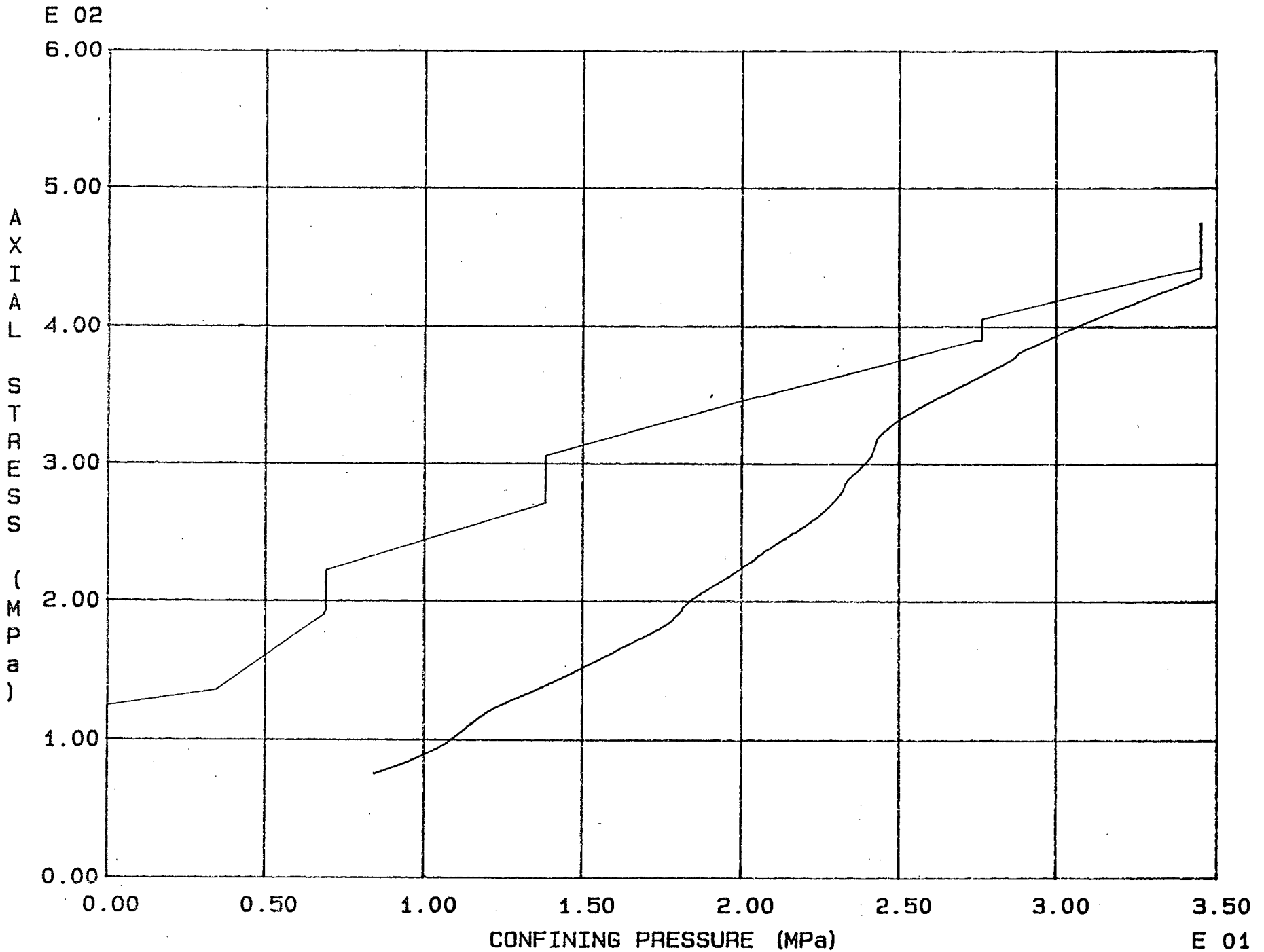

Fig. D - 2 Specimen G20

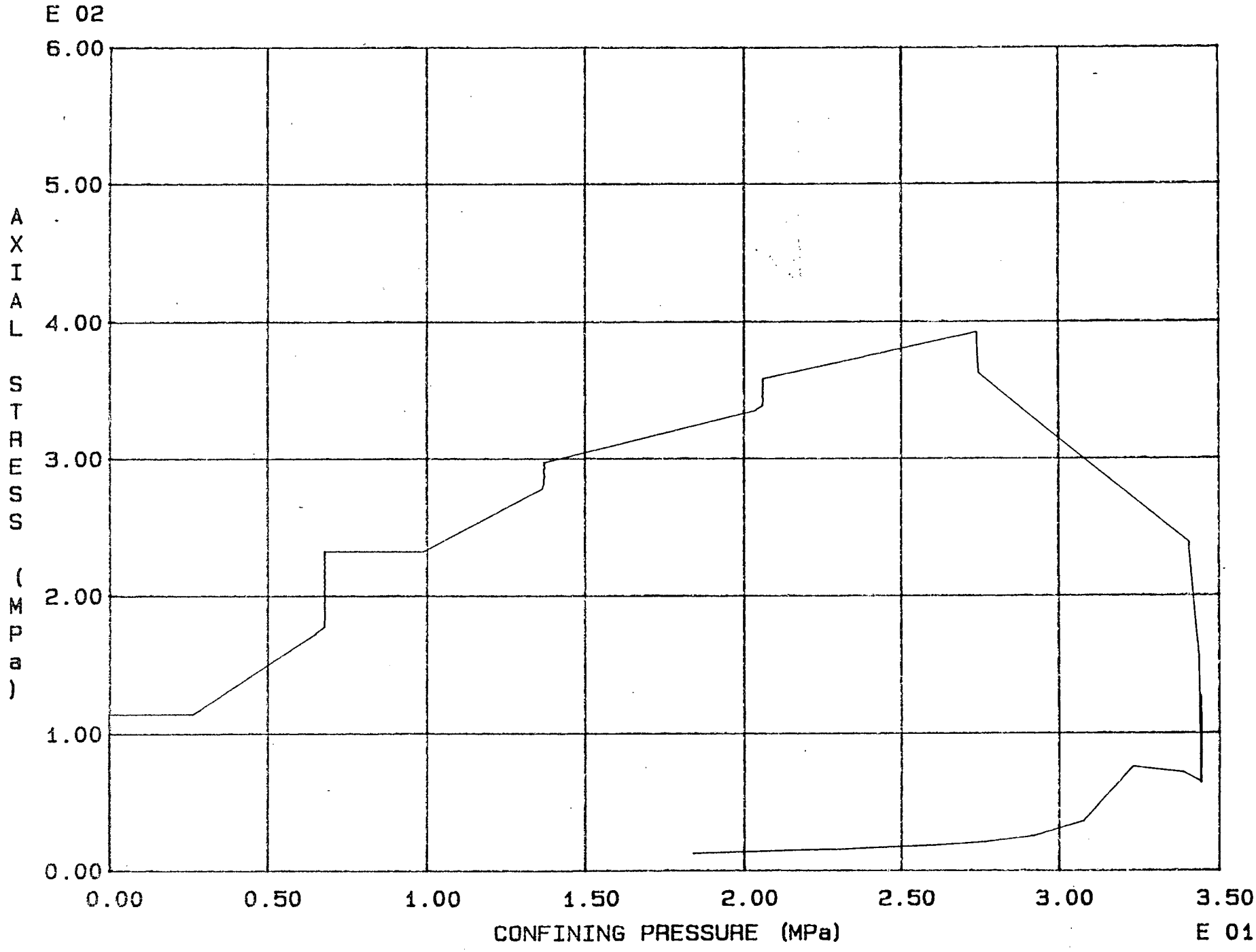

Fig. D - 4 Specimen G22

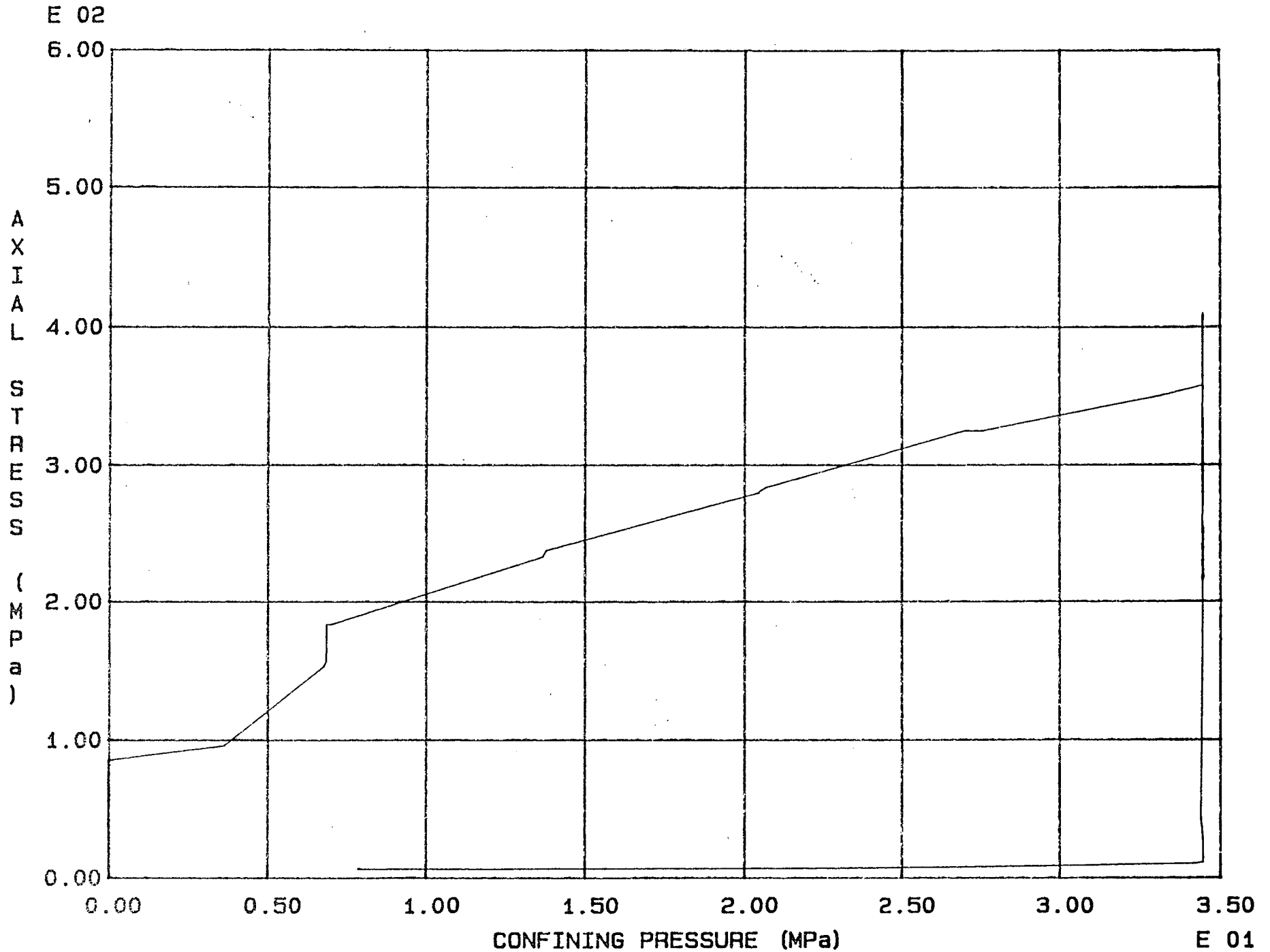

Fig. D - 6 Specimen G24

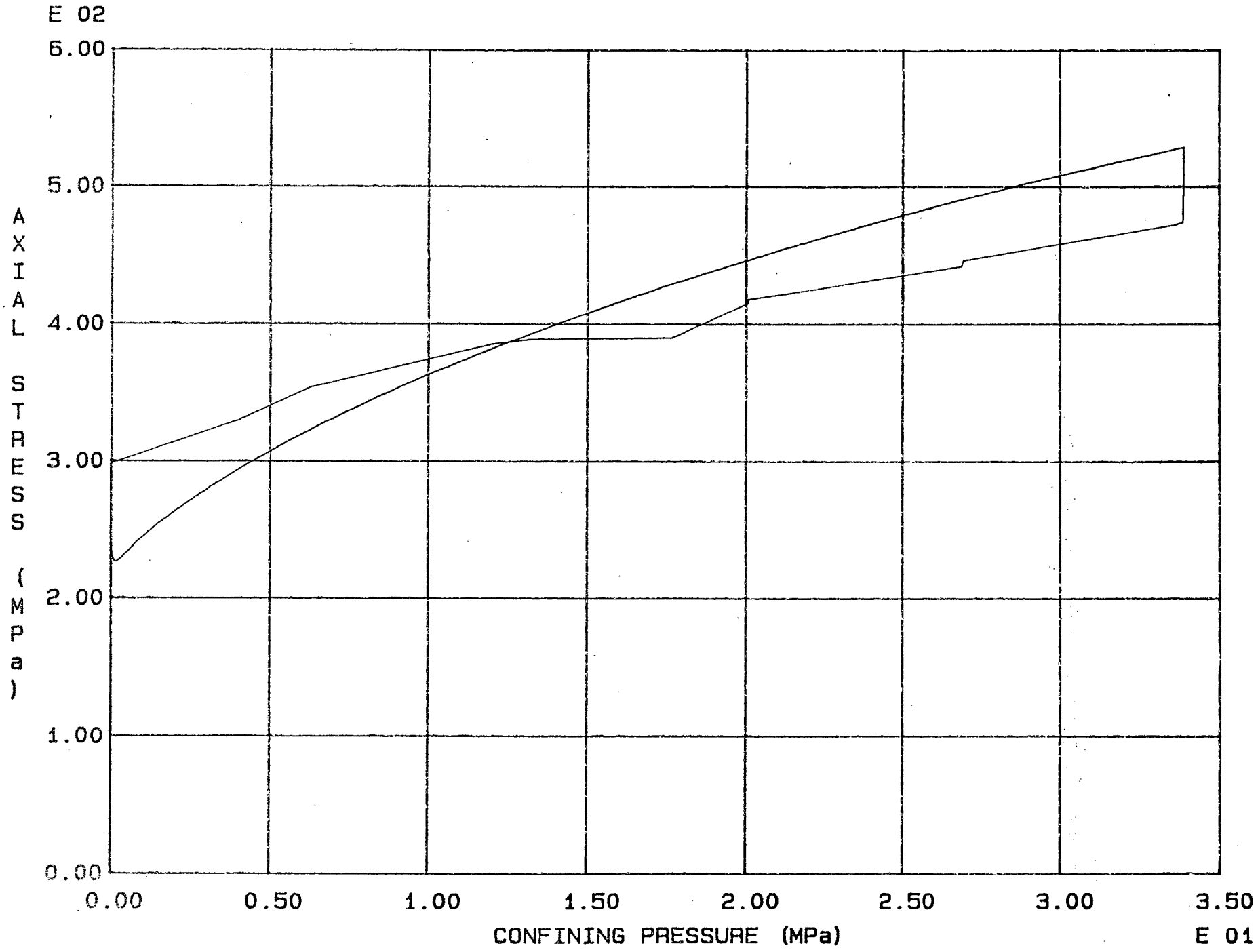

Fig. D - 8 Specimen D26